Journal of Geodynamics 119 (2018) 221–241

Contents lists available at ScienceDirect

Journal of Geodynamics

journal homepage: www.elsevier.com/locate/jog

Late Paleozoic – Mesozoic tectonic evolution of the Eastern Taimyr-Severnaya Zemlya Fold and Thrust Belt and adjoining Yenisey-Khatanga Depression

Andrey K. Khudoley[a,*], Vladimir E. Verzhbitsky[b], Dmitry A. Zastrozhnov[c,d], Paul O'Sullivan[e], Victoria B. Ershova[a], Vasily F. Proskurnin[c], Marianna I. Tuchkova[f], Mikhail A. Rogov[f], T. Kurtis Kyser[g,1], Sergey V. Malyshev[a], Gennady V. Schneider[c]

[a] Institute of Earth Sciences, St. Petersburg State University, 7/9 University Nab., St. Petersburg, 199034, Russia
[b] Shirshov Institute of Oceanology RAS, Nakhimovski Pr., 36, Moscow, 117997, Russia
[c] A.P. Karpinsky Russian Geological Research Institute (VSEGEI), Sredniy Prospect 74, St. Petersburg, 199106, Russia
[d] Centre for Earth Evolution and Dynamics (CEED), University of Oslo, Oslo, N-0315, Norway
[e] GeoSep Services,1521 Pine Cone Road, Moscow, ID, 83843, USA
[f] Geological Institute, Russian Academy of Science, Pyzhevsky Per. 7, Moscow, 119017, Russia
[g] Department of Geological Sciences and Geological Engineering, Queen's University, Kingston, ON, K7L 3N6, Canada

ARTICLE INFO

Keywords:
Arctic
Taimyr-Severnaya Zemlya fold and thrust belt
Structural geology
Apatite fission track data
Ar-Ar muscovite dating
U-Pb granite dating
Tectonic evolution

ABSTRACT

Combined structural, thermochronological and geochronological studies were carried out to unravel the complex late Paleozoic – Mesozoic tectonic evolution of the eastern Taimyr – Severnaya Zemlya Fold and Thrust Belt, along with the adjoining Yenisey-Khatanga Depression and Olenek Fold Zone. New detailed field mapping, a fault and fold geometry and kinematic study, and paleostress reconstruction were undertaken for key areas within the Central and Southern Taimyr domains and the Olenek Fold Zone. Thirty seven samples were used for apatite fission track (AFT) analysis along with two samples for U-Pb zircon granite dating, and three samples for Ar-Ar metamorphic muscovite dating.

The late Paleozoic (Early Carboniferous – Permian) tectonic event is recognized only in a relatively narrow zone including the Northern Taimyr Domain and part of the Central Taimyr Domain. It started in the Early Carboniferous (Visean) and is synchronous with the earliest stages of collision in the Uralian Orogen. Our results reveal a widespread distribution of latest Triassic – earliest Jurassic and Cretaceous deformations. The latest Triassic – earliest Jurassic tectonic event significantly overprinted the Northern and Central Taimyr domains and original unaltered late Paleozoic AFT ages are identified only locally. New completely reset AFT cooling ages group at 195-180 Ma, in reasonable agreement with structural data. Older Neoproterozoic and late Paleozoic Ar-Ar ages of metamorphic muscovite are retained, demonstrating that the dated rocks were not heated above 300 °C. An Early Cretaceous tectonic event is inferred from both the structural study and ca. 115–125 Ma AFT cooling ages, and is most widespread in the Southern Taimyr Domain, Olenek Fold Zone and adjoining parts of the Yenisey-Khatanga Depression, modifying older geological structures. A younger Late Cretaceous tectonic event at ca. 100-60 Ma is also inferred from AFT cooling ages, but its distribution is poorly constrained.

Our study reveals that the distribution of late Mesozoic tectonic events has been significantly underestimated in previous structural studies of the region. The latest Triassic – earliest Jurassic and Cretaceous tectonic events are easily correlated with those in the Pai-Khoi – Novaya Zemlya and northern Verkhoyansk fold and thrust belts.

1. Introduction

The Taimyr-Severnaya Zemlya Fold and Thrust Belt (TSZ) is located along the northern margin of the Siberian Craton and is a key structural element for understanding the tectonic evolution of the circum-Arctic area, and relationship between the Pai-Khoi – Novaya Zemlya,

* Corresponding author.
E-mail address: a.khudoley@spbu.ru (A.K. Khudoley).
[1] Deceased 29 August 2017.

https://doi.org/10.1016/j.jog.2018.02.002
Received 15 August 2017; Received in revised form 29 January 2018; Accepted 17 February 2018
Available online 23 February 2018
0264-3707/

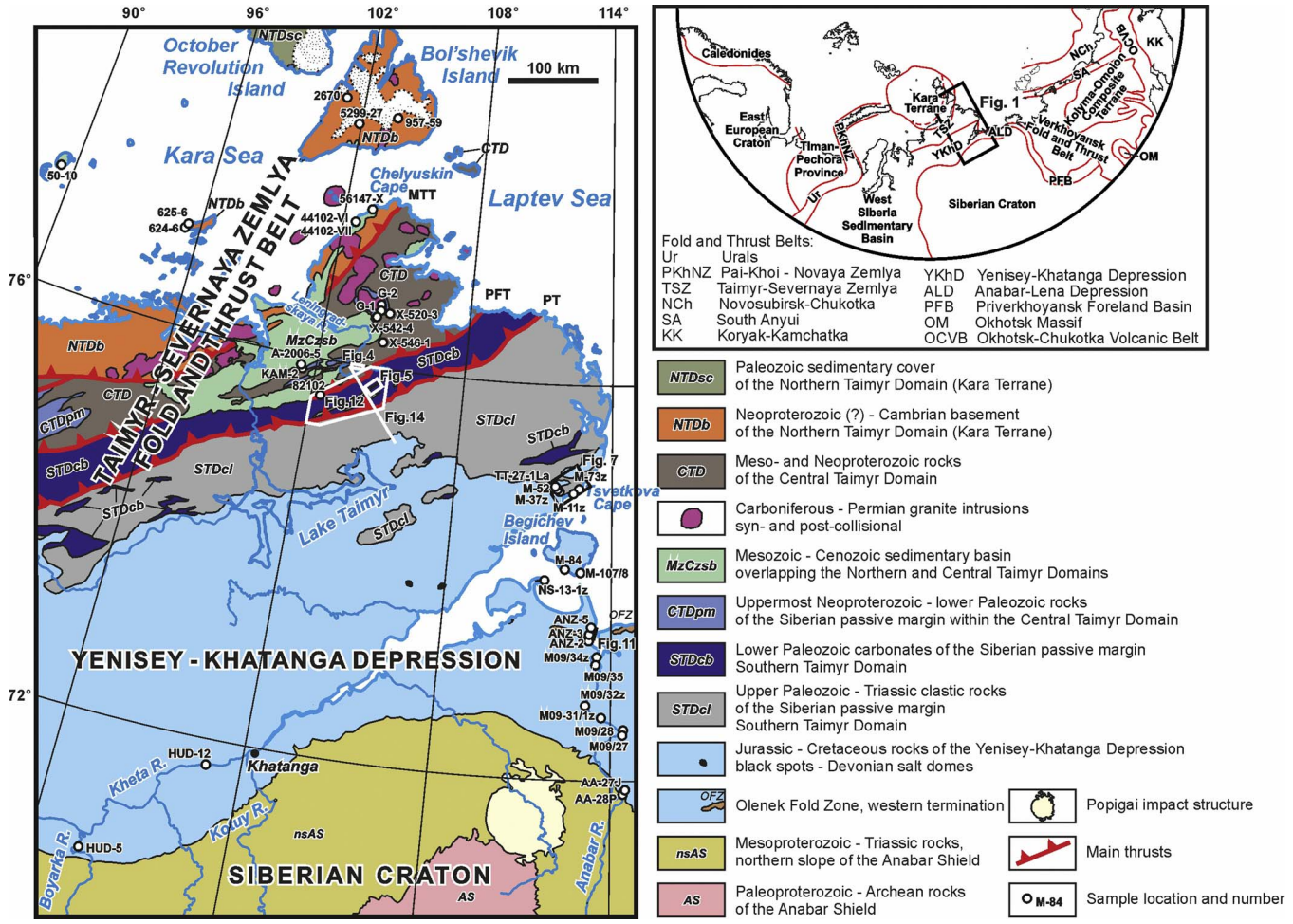

Fig. 1. Tectonic map showing location of the main tectonic domains, key areas and cross-sections, and studied samples. MTT – Main Taimyr Thrust, PFT – Pyasino-Faddey Thrust, PT – Pogranichniy Thrust. Sample 102-4 located outside the map on the Izvestiy TSIK Islands (see Suppl. 1 for coordinates).

Verkhoyansk and South Anyui fold and thrust belts (Pease, 2011; Drachev, 2011, 2016 and references therein) (Fig. 1). The TSZ shows evidence for several tectonic events, with the most extensive deformations in the Neoproterozoic and late Paleozoic – Mesozoic. Numerous studies utilizing isotopic, geochemical and paleomagnetic techniques, along with recent field mapping, have significantly improved our knowledge of the Neoproterozoic tectonic evolution of the TSZ (Vernikovsky and Vernikovskaya, 2001; Pease et al., 2001; Vernikovsky et al., 2004, 2011; Lorenz et al., 2008; Pease and Scott, 2009; Makariev and Makarieva, 2011; Makariev, 2013; Metelkin et al., 2012; Priyatkina et al., 2017). By contrast, the late Paleozoic – Mesozoic tectonic evolution of the region is much more poorly understood; so much so that even the timing of tectonic deformation is poorly constrained throughout the region (Zonenshain et al., 1990; Uflyand et al., 1991; Vernikovsky, 1996; Vernikovsky et al., 1998; Inger et al., 1999; Pease, 2011). The Olenek Fold Zone (Olenek FZ) represents the western continuation of the Verkhoyansk Fold and Thrust Belt (Verkhoyansk FTB) and is likely linked with the Southern Taimyr Domain, but is very poorly studied (Prokopiev and Deikunenko, 2001; Drachev and Shkarubo, 2018). Numerous seismic studies performed over the past 10 years have significantly improved our knowledge of the Yenisey-Khatanga Depression structure, but its tectonic evolution is still under discussion (Kontorovich, 2011; Pronkin et al., 2012; Afanasenkov et al., 2016).

Until this study, the only published interpretation of the exhumation and cooling history of the TSZ was based on apatite fission track (AFT) results presented by Zhang et al. (2018). This paper provides better constraints on the timing of the late Paleozoic – Mesozoic deformation events and the relationship of these events to other fold and thrust belts in the Arctic realm. This is accomplished by integrating results of (1) recently-completed geological mapping and structural studies throughout the TSZ that better define the relationships between different structural domains and allows for paleostress reconstructions; and (2) extensive geochronologic and thermochronologic dating program using rock samples collected from throughout the eastern part of the TSZ and adjoining Yenisey-Khatanga Depression and Olenek FZ.

2. Geological setting

The study area includes the TSZ, Yenisey-Khatanga Depression and the westernmost part of the Olenek FZ (Fig. 1). The TSZ comprises sedimentary, magmatic and metamorphic rocks varying in age from Neoproterozoic to Cretaceous. According to Zonenshain et al. (1990), Uflyand et al. (1991) and Vernikovsky (1996), three SW-NE-trending structural domains with distinct stratigraphic, magmatic and tectonic histories are identified.

The Northern Taimyr Domain includes the northern part of the Taimyr Peninsula which, together with the Severnaya Zemlya archipelago, represents the highly deformed and metamorphosed southeast margin of a large cratonic block commonly known as the Kara Microcontinent, Kara Terrane or Kara Plate (Vernikovsky, 1996; Vernikovsky and Vernikovskaya, 2001; Metelkin et al., 2005; Ershova et al., 2015b) (Fig. 1). Most of the Kara Terrane is now hidden below the Kara Sea (Drachev, 2011, 2016 and references therein). The

Northern Taimyr Domain consists of clastic rocks interpreted as continental slope turbidites, which were metamorphosed to greenschist and amphibolite facies. Based on recent U-Pb detrital zircon data and mapping results, most metamorphic rocks are Cambrian in age and not Proterozoic as previously supposed (Zonenshain et al., 1990; Pogrebitsky and Shanurenko, 1998; Lorenz et al., 2008; Pease and Scott, 2009; Makariev and Makarieva, 2011; Makariev, 2013; Ershova et al., 2015c). The southern boundary of the North Taimyr Domain in eastern Taimyr is marked by faults of the Main Taimyr Thrust zone, with both thrust and dextral strike-slip kinematics (Bezzubtsev et al., 1986; Vernikovsky 1996; Metelkin et al., 2005; Makariev and Makarieva, 2011). In the northern part of the domain, across October Revolution Island, the Ordovician and younger Paleozoic sedimentary rocks are characterized by sub-horizontal bedding forming sedimentary cover of the Kara Terrane. Further south on Bol'shevik Island, the lower Paleozoic sedimentary cover is eroded and the oldest unmetamorphosed sedimentary rocks are Upper Carboniferous to Lower Permian locally distributed and moderately deformed clastic rocks (Makariev and Makarieva, 2011; Ershova et al., 2015b).

The Central Taimyr Domain is also known as the Central Taimyr accretionary belt (Vernikovsky and Vernikovskaya, 2001). It consists of Meso- and Neoproterozoic clastic and carbonate rocks, ophiolite, and magmatic rocks of different tectonic settings metamorphosed from greenschist to amphibolite facies and overlain by an Ediacaran to mid-Silurian predominantly shaley succession (Fig. 1). Ages of the magmatic rocks vary from 1365 ± 11 Ma to 617 ± 4 Ma (Makariev, 2013; Priyatkina et al., 2017). U-Pb detrital zircon study of the quartzite unit at the top of the sedimentary succession shows that 12 out of 100 dated grains form a ca. 600 Ma peak, pointing to the minimum depositional age of the quartzite unit (Makariev, 2013). Garnet-amphibolite metamorphism, associated with ophiolite obduction, occurred at ca. 626–575 Ma (Vernikovsky et al., 2004). Erosional products of the Central Taimyr Domain have been identified by U-Pb detrital zircon studies in Ediacaran to Cambrian clastic rocks throughout the northern part of the Siberian Craton (Khudoley et al., 2015; Kuptsova et al., 2015; Priyatkina et al., 2017).

Abundant syn-collisional granite intrusions ranging in age from 344 to 275 Ma, cut clastic rocks in the northern part of the Taimyr Peninsula (Vernikovsky, 1996; Makariev, 2013). The number of intrusions decreases northward and on Bol'shevik Island they have only a limited distribution (Fig. 1). Both the Northern and Central Taimyr domains are cut by ca. 265-250 Ma granite intrusions forming stitching plutons (Vernikovsky et al., 1998).

Jurassic and Lower Cretaceous clastic rocks are characterized by sub-horizontal bedding and overlie older units in both the Northern and Central Taimyr domains, with a major angular unconformity at the base. Makariev (2013) reported a limited distribution of Middle-Upper Triassic clastic rocks in the Central Taimyr Domain, but ages of these rocks are based on poorly fossilized flora and require further study.

The Southern Taimyr Domain consists of latest Neoproterozoic (Ediacaran) to Triassic sedimentary rocks, and represents the north-west facing ancient passive margin of the Siberian continent, in modern coordinates (Uflyand et al., 1991; Vernikovsky, 1996) (Fig. 1). The Middle Carboniferous – Permian part of the sedimentary succession contains numerous dolerite sills, which, along with basalts and tuffs of different composition in the lowermost Triassic rock units and similarly aged felsic intrusions, are linked to Siberian Trap magmatism (Vernikovsky et al., 2003). Towards the north-west, the Upper Cambrian – Silurian sedimentary rocks display a transformation from a thick carbonate succession to transitional carbonate-shale and relatively thin shale successions (Fig. 2). To the west from the study area, a similar facies transition has been documented for Devonian and Lower Carboniferous sedimentary rocks as well (Ershova et al., 2016a and references therein). The shale succession is widespread in the Central Taimyr Domain, showing that during the Cambrian − Early Carboniferous, this domain represented a distal part of the Siberian passive margin. The provenance of Middle Carboniferous – Permian clastic rocks has traditionally been attributed to erosion of the late Paleozoic Taimyr Orogen (Vernikovsky, 1996; Pogrebitsky and Shanurenko, 1998; Proskurnin, 2009b), however, recent U-Pb detrital zircon studies suggest a number of provenances for the clastics, probably including the Uralian Orogen and the Central Asian Orogenic Belt (Zhang et al., 2013, 2016; Ershova et al., 2015a, 2016b).

The boundary between the Central and Southern Taimyr domains is mainly represented by the Pyasino-Faddey Thrust, but an unconformable relationship between metamorphic rocks of the Central Taimyr Domain and overlying Ediacaran – lower Paleozoic passive margin succession of the Southern Taimyr Domain has also been documented (Fig. 3). Areas with a predominant distribution of lower Paleozoic carbonate rocks and upper Paleozoic – Triassic clastic rocks are separated by the Pogranichniy Thrust (Vernikovsky, 1996; Proskurnin, 2009a,b).

The Yenisey-Khatanga Depression separates thick Paleozoic rock units of the Southern Taimyr Domain from much thinner and stratigraphically incomplete Paleozoic rocks of the central part of the Siberian Craton (Fig. 1). Total thickness of Jurassic and Cretaceous rocks reaches 10–11 km in the central part of the depression, decreasing towards its margins and north-eastward (Afanasenkov et al., 2016). Sub-horizontal bedding is typical across much of the depression, although low-angle arches have been seismically mapped (Kontorovich, 2011; Pronkin et al., 2012; Afanasenkov et al., 2016). Steeply dipping bedding is only documented in association with Devonian salt diapirs, which have pierced to the surface in the eastern part of the depression (Pogrebitsky and Shanurenko, 1998; Pronkin et al., 2012; Afanasenkov et al., 2016). A large shallow anticline cored by Triassic rocks in the easternmost part of the Yenisey-Khatanga Depression represents the western termination of the Olenek FZ (Fig. 1). The latter is exposed along the southern coast of the Laptev Sea and forms a western branch of the Verkhoyansk FTB, changing its strike in the vicinity of the Lena Delta and continuing up to the eastern coast of the Taimyr Peninsula and offshore below the Laptev Sea sedimentary basin (Prokopiev and Deikunenko, 2001; Drachev, 2011; Drachev and Shkarubo, 2018).

Jurassic and Cretaceous rocks of the Yenisey-Khatanga Depression unconformably overlie upper Paleozoic and Triassic rocks of the Southern Taimyr Domain, which are locally exposed in the core of uplifted blocks along the northern margin of the basin (Fig. 1). The unconformity is clearly recognized on maps and seismic profiles (Pogrebitsky and Shanurenko, 1998; Proskurnin, 2009a; Pronkin et al., 2012; Afanasenkov et al., 2016; Zhang et al., 2018). Several local unconformities are also recognized within the Jurassic-Cretaceous succession.

3. Structural geology

In the Central and Southern Taimyr domains, the predominant structures are NE-trending thrusts and folds recognized on maps of different scales (e.g. Bezzubtsev et al., 1983; Pogrebitsky, 1998; Proskurnin, 2009a; Makariev and Makarieva, 2011; Proskurnin et al., 2016). Several important questions regarding the structural geology, such as the relationship between SE- and NW-vergent structures, distribution and sense of displacement along strike-slip faults, and thin-skinned versus thick-skinned tectonics, are still under discussion (e.g. Vernikovsky 1996; Inger et al., 1999; Metelkin et al., 2005; Zhang et al., 2016). The key areas exposing the different structural styles are discussed below.

3.1. Svetliy Creek area

The Svetliy Creek area is located in the NW part of the Central Taimyr Domain (Fig. 1), where the contact between metamorphosed clastic and carbonate rocks of the Mesoproterozoic Zhdanov Formation (Fm) and unmetamorphosed clastic rocks of the Neoporoterozoic

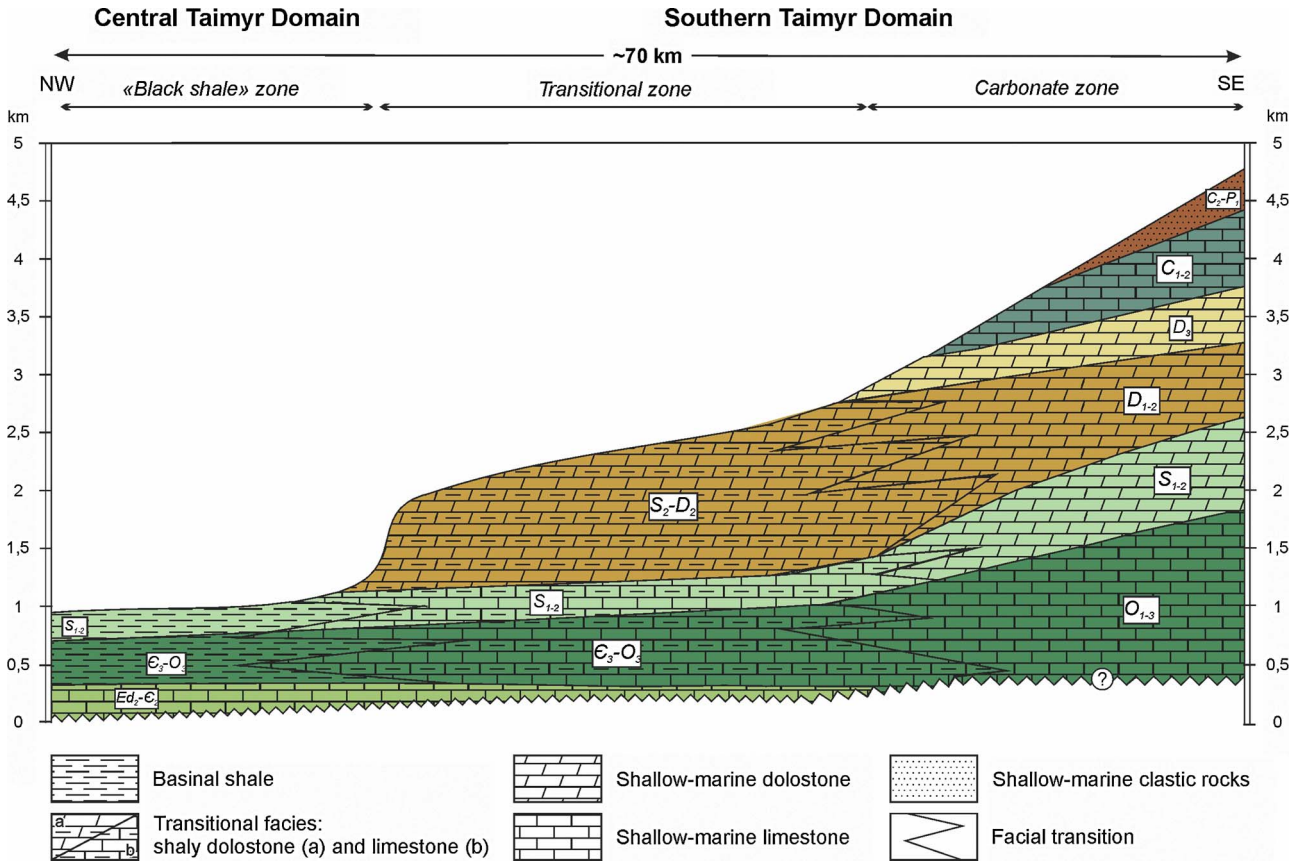

Fig. 2. Cross-section showing Paleozoic facies transition. Location of the main facies zones shown with reference to modern structure and not palinspastically restored. Note that shale basin of the Siberian passive margin overlaps the Central Taimyr Domain.
Data Source: Pogrebitsky and Shanurenko (1998); Proskurnin (2009b), Makariev (2013) and observations by authors.

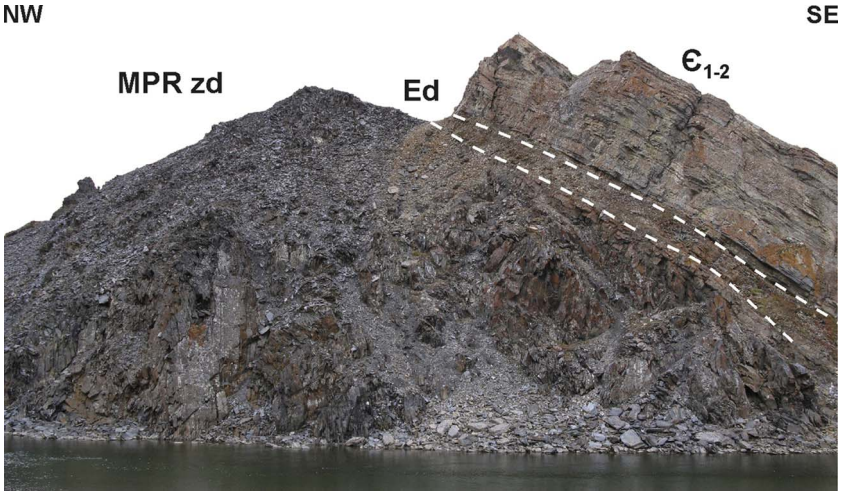

Fig. 3. Unconformity between Mesoproterozoic metamorphic rocks of the Zhdanov Fm (MPR zd) and overlying Ediacaran (Ed) – Cambrian ($Є_{1-2}$) passive margin succession. Cliff is approximately 40 m high. Central Taimyr Domain, Korallovaya River, photo by A.A.Bagaeva.

Stanovskaya Fm (Fig. 4) is exposed. A Mesoproterozoic age of the Zhdanov Fm here is supported by U-Pb baddeleyite dating of mafic sills at 1345 ± 35 and 1365 ± 11 Ma, whereas the Stanovskaya Fm contains detrital zircons as young as ca. 760–765 Ma (Priyatkina et al., 2017).

The Stanovskaya Fm typically consists of 3 units: light-gray to greenish-gray sandstone with conglomerate interbeds (lower), variegated shale with sandstone interbeds (middle), and red sandstone with shale interbeds (upper) (Makariev, 2013). In the Svetliy Creek area, the lower unit is truncated by a fault and the Mesoproterozoic rocks are in direct contact with the middle unit (Fig. 4). Based on field observations, the fault is a SE-dipping thrust that cuts bedding in the footwall and tight to isoclinal folds in the hanging wall (Fig. 4a,b), suggesting its formation post-dates the tectonic events which resulted in folding of the Zhdanov and Stanovskaya formations. SE-dipping thrusts were also mapped to the north-east of the study area by Samygin (2012, 2015).

Numerous small faults with slickenlines were studied in the

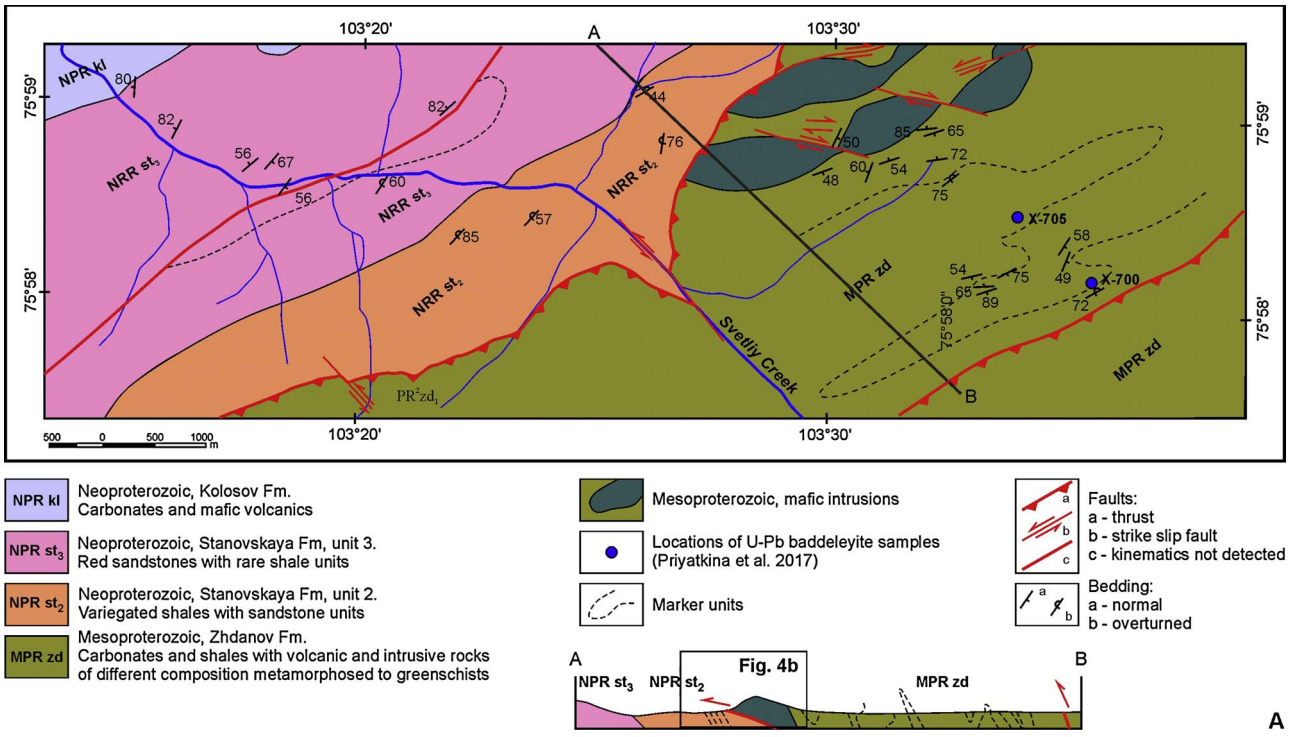

Fig. 4. Svetliy Creek key area showing NW-vergent thrust of Mesoproterozoic magmatic and metamorphic rocks of the Zhdanov Fm above Neoproterozoic sandstones of the Stanovskaya Fm. A – geological map and cross-section. Note location of mafic sills with U-Pb baddeleyite age 1365 ± 11 (X-705) and 1345 ± 35 (X-700) (Priyatkina et al., 2017) supporting Mesoproterozoic age of host rocks. B – contact between Mesoproterozoic Zhdanov Fm including mafic intrusion and Neoproterozoic Stanovskaya Fm. Sandstone and shale of the Stanovskaya Fm are in overturned bedding. C – Stress field restoration based on study of small faults with slickenlines. N – number of measurements. Arrows show hanging wall slip direction inferred by slickenline orientation and predominantly calcite slickenfibers. Schmidt net, lower hemisphere. σ_1–axis of compression, σ_2–intermediate axis, σ_3–axis of tension. Stress axes were calculated using FaultKin software (Marrett and Allmendinger, 1990; Allmendinger et al., 2012). Note that compression and tension axes calculated for thrusts approximately parallel to tension and compression axes calculated for normal faults correspondently. See Fig. 1 for location.

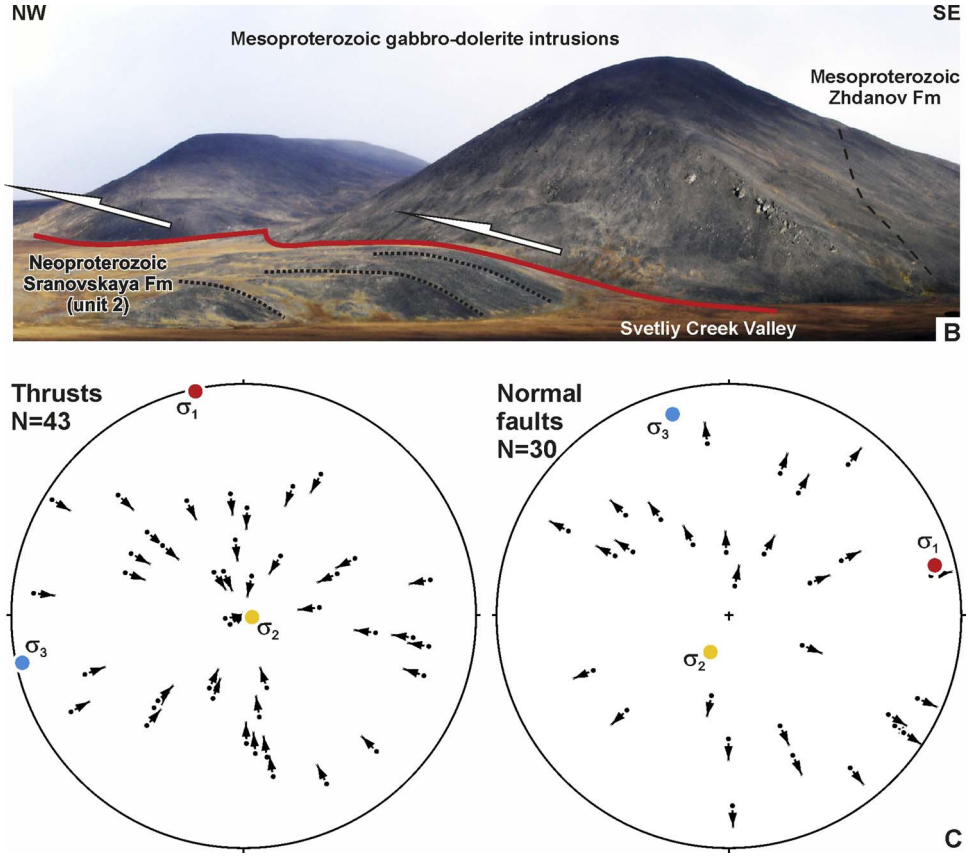

Fig. 4. (*continued*)

northern part of the Svetliy Creek area, in both magmatic and metasedimentary rocks of the Mesoproterozoic Zhdanov Fm (Fig. 4c). Dip-slip displacement predominates in 49 out of 84 faults, and thrusts predominate over normal faults. Almost all faults have a strike-slip component of displacement, and dextral and sinistral strike-slip faults have an approximately equal distribution. Normal faults cross cut thrusts showing that they were formed during different tectonic events and, therefore, we made an initial fault data separation into 2 populations with thrust and normal components of displacement respectively. The thrust fault-related stress field has a sub-horizontal compression axis trending at approximately 350°, and sub-vertical tension axis, whereas the normal fault-related stress field has an almost opposite orientation of stress axes, with a tension axis trending at approximately 345° and a sub-vertical compression axis (Fig. 4c).

3.2. Podkhrebetnaya River area

The Podkhrebetnaya River area is located within the Southern Taimyr Domain near the contact between lower Paleozoic shallow-marine carbonates and carbonate-shale basinal facies (Fig. 1). The Podkhrebetnaya River area is composed of Paleozoic rocks ranging in age from Ordovician to Permian and forming a regional-scale SE-vergent syncline (Fig. 5). In the NW part of the study area, Silurian shale and carbonate rock units are separated from Devonian shallow-marine carbonates by a low-angle NW-dipping thrust. A slice of Devonian carbonates with overturned bedding is in turn thrust onto Upper Carboniferous – Lower Permian clastic rocks. In the south-east part of the Podkhrebetnaya River area, a NW-dipping thrust separating shallow-marine carbonates of Ordovician and Devonian – Carboniferous ages has been mapped. All thrusts of the Podkhrebetnaya River area are approximately parallel to bedding in the hanging wall, suggesting that thrusts and folds were likely formed during the same tectonic event. Small E-W-trending dextral and NNW-trending sinistral strike-slip faults with an offset of less than 300 m, cutting rock units in the core and on the limb of regional-scale synclines, have been mapped throughout the Podkhrebetnaya River area.

All stratigraphic units on the map are parallel to each other, suggesting an absence of unconformities in the Ordovician – Lower Permian succession. Significant variation of bedding dips near thrust planes makes the total distribution of poles to bedding quite complicated (Fig. 6). However, axes of small folds are oblique to the main structural trend, forming an angle of up to 50° in a counterclockwise direction with respect to the average structural trend (Fig. 6).

3.3. Tsvetkova Cape area

The Tsvetkova Cape area is located on the southern margin of the Southern Taimyr Domain, where Jurassic and younger rocks of the Yenisey-Khatanga Depression unconformably overlie pre-Jurassic rocks of the domain (Fig. 1). The Tsvetkova Cape area contains exposures of clastic rocks ranging in age from Permian to Jurassic. Mapping and detailed paleontological studies show the occurrence of localized erosion and several hiatuses in Triassic strata, but the only regional-scale unconformity has been documented at the base of the Jurassic (Fig. 7) (Migai, 1952; Dagys and Kazakov, 1984; Pogrebitsky, 1998; Pogrebitsky and Shanurenko, 1998; Proskurnin, 2009b). Near

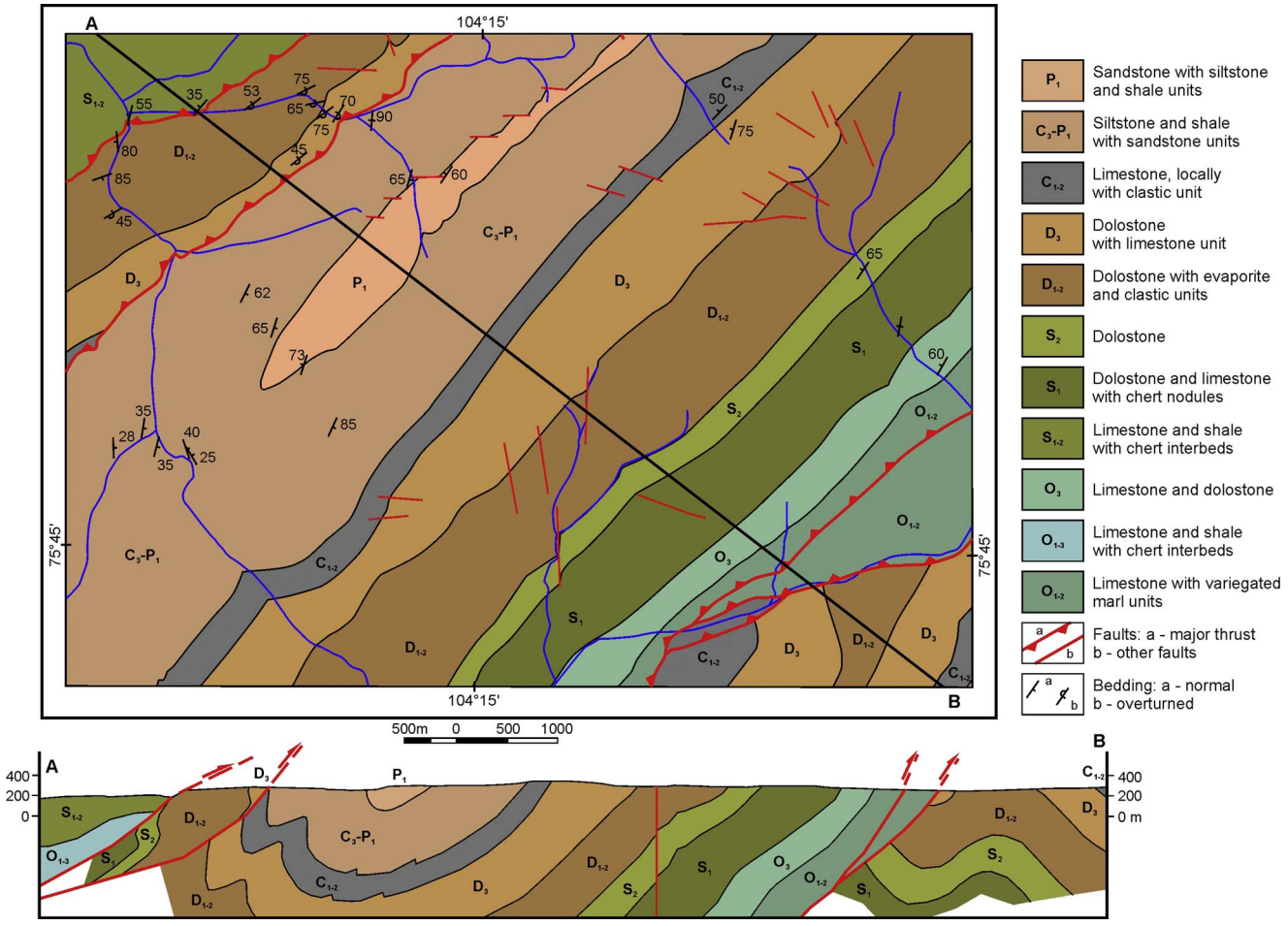

Fig. 5. Geological map and cross-section via the Podkhrebetnaya River key area showing structural style of the Southern Taimyr Domain. Note bedding-parallel SE-vergent thrusts in NW and SE parts of the study area. See Fig. 1 for location.

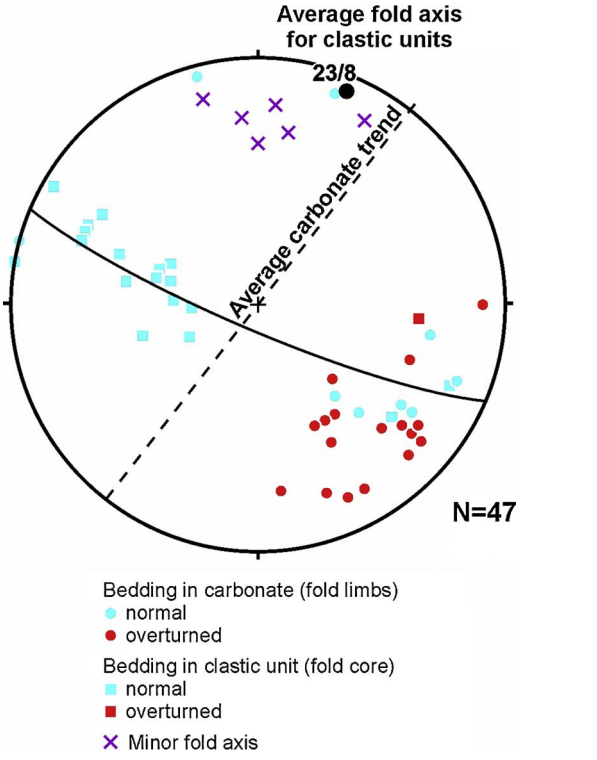

Fig. 6. Pole to bedding and minor folds axes plot for the Podkhrebetnaya River area, Schmidt net, lower hemisphere. Average fold axis was only estimated by clastic rocks bedding. Note oblique relationship between average trend of carbonates on the fold limb, average fold axis of clastic rocks and axes of small folds, interpreted as resulted from strike slip displacement.

Tsvetkova Cape, approximately 600 m of the Upper and Middle Triassic rocks were eroded beneath Jurassic strata and the restored average dip of beds in pre-Jurassic time was close to 7°. However, dips of Jurassic rocks in the Tsvetkova Cape area locally exceed 40°, suggesting that post-Jurassic folding was more intense than the pre-Jurassic in this area (Fig. 7). To the south-west of the Tsvetkova Cape area, Jurassic rocks dip at a very gentle angle and an unconformity at the base of Jurassic rocks is clearly recognized on geological maps (e.g. Pogrebitsky, 1998; Proskurnin, 2009a; Proskurnin et al., 2016). A low-angle unconformity at the base of Jurassic rocks has also been identified by seismic studies within the Yenisey-Khatanga Depression (Kontorovich, 2011; Pronkin et al., 2012; Afanasenkov et al., 2016).

Although in the Southern Taimyr Domain folds are typically upright or SE-vergent and deformation decreases south-eastward, in the Tsvetkova Cape area there are two NW-vergent folds with a bedding dip as high as 70° (Fig. 7). Small folds are widely distributed in Permian rocks in the core of regional-scale anticline and in shear zones on its limbs. Axes of small folds are almost parallel to the mean axis of the regional-scale folds.

Numerous small faults with slickenlines were documented throughout the Tsvetkova Cape area, in rocks varying in age from Permian to Middle Jurassic, with 205 faults studied in total. Faults with a predominance of dip-slip and strike slip displacement have an approximately similar distribution. Faults with thrust (109 out of 205) and dextral (118 out of 205) components of displacement predominate. Similar to the Svetliy Creek area, normal faults cut thrust faults and our initial fault data was separated into 2 populations with thrust and normal components of displacement respectively. The stress field estimated by faults with a thrust component of displacement displays a N-trending compression axis and sub-vertical tension axis, whereas the stress field estimated by faults with a normal component of displacement displays an approximately 350°-trending tension axis and sub-vertical compression axis (Fig. 8). Stress fields restored by faults with a thrust component of displacement distributed in Permian-Triassic and Lower-Middle Jurassic rocks display a very similar orientation of stress axes, suggesting that all faults with a thrust component of displacement were formed by the same stress field in post-Middle Jurassic time.

3.4. NW-vergent structures

All published maps and cross-sections across the TSZ display only sub-vertical or SE-vergent thrusts and folds (Pogrebitsky, 1971, 1998; Bezzubtsev et al., 1983; Inger et al., 1999; Vernikovsky and Vernikovskaya, 2001; Proskurnin, 2009a; Makariev and Makarieva, 2011; Zhang et al., 2018). Localized distribution of NW-vergent structures, especially in the Central Taimyr Domain, was also documented (Pease, 2011; Samygin, 2012, 2015; Priyatkina et al., 2017). Our study shows that NW-vergent structures of different scales are widely distributed in the Central and Southern Taimyr domains. Regional-scale NW-vergent thrusts and tight to isoclinal folds have been mapped in the northern part of the Central Taimyr Domain (Fig. 4). Regional-scale NW-vergent folds have also been found in the Tsvetkova Cape area (Fig. 7), located on the southern margin of the Southern Taimyr Domain.

Small NW-vergent thrusts and folds have been documented throughout the Southern Taimyr Domain in both clastic and carbonate rocks of widely varying ages (Fig. 9). Bedding-parallel thrusts with hanging wall anticlines are widespread and most typical for the northern part of the Southern Taimyr Domain, within the transitional zone between lower Paleozoic carbonate and shale rock units (Fig. 9a). Thrusts with well-preserved flat-and-ramp geometry were only found in Triassic rocks in cliffs on the Laptev Sea coast near Tsvetkova Cape (Fig. 9b), but are likely to have a much more widespread distribution and have not been documented due to poor-quality exposures inland away from the coast.

3.5. Strike-slip displacements

Dextral strike-slip faults are often reported from the eastern TSZ, but no outcrop-scale structures supporting dextral displacement have been described (Pogrebitsky, 1971, 1998; Inger et al., 1999; Metelkin et al., 2005; Proskurnin, 2009b). At the map scale, E-W-trending dextral strike-slip faults with offsets of a few kilometers were documented throughout the Southern Taimyr Domain. They cut obliquely through NE-trending structures, suggesting that they post-date the formation of regional-scale thrusts and faults (Fig. 10a). The en-echelon array of folds is locally recognized and their geometric relationship with bounding thrusts may also be interpreted as evidence for dextral strike-slip displacement along them (Fig. 10a).The oblique relationship between axes of small and regional-scale folds in the Podkhrebetnaya River area (Fig. 6) may be attributed to dextral displacement as well.

Our study in the Svetliy Creek area of the Central Taimyr Domain (Fig. 4) and Tsvetkova Cape area in the Southern Taimyr Domain (Fig. 8) reveals the occurrence of both dextral and sinistral strike-slip faults, with dextral strike-slip faults being more widespread. Both dextral and sinistral strike-slip faults were mapped in the Podkhrebetnaya River area (Fig. 5). The relationship between orientations of compression axes estimated in the Svetliy Creek and Tsvetkova Cape areas, and major thrusts provides evidence that thrust faults experienced sinistral displacement (Fig. 10b).

3.6. Anabar Bay area

The Anabar Bay area is located at the western termination of the Olenek FZ (Fig. 1) and consists of clastic rocks varying in age from Triassic to Early Cretaceous. The predominant structure is a broad anticline with beds dipping to the north and south at less than 10° (Fig. 11). Near its termination, the Olenek FZ forms a kink represented by variation in the average trend of the regional-scale fold axis from

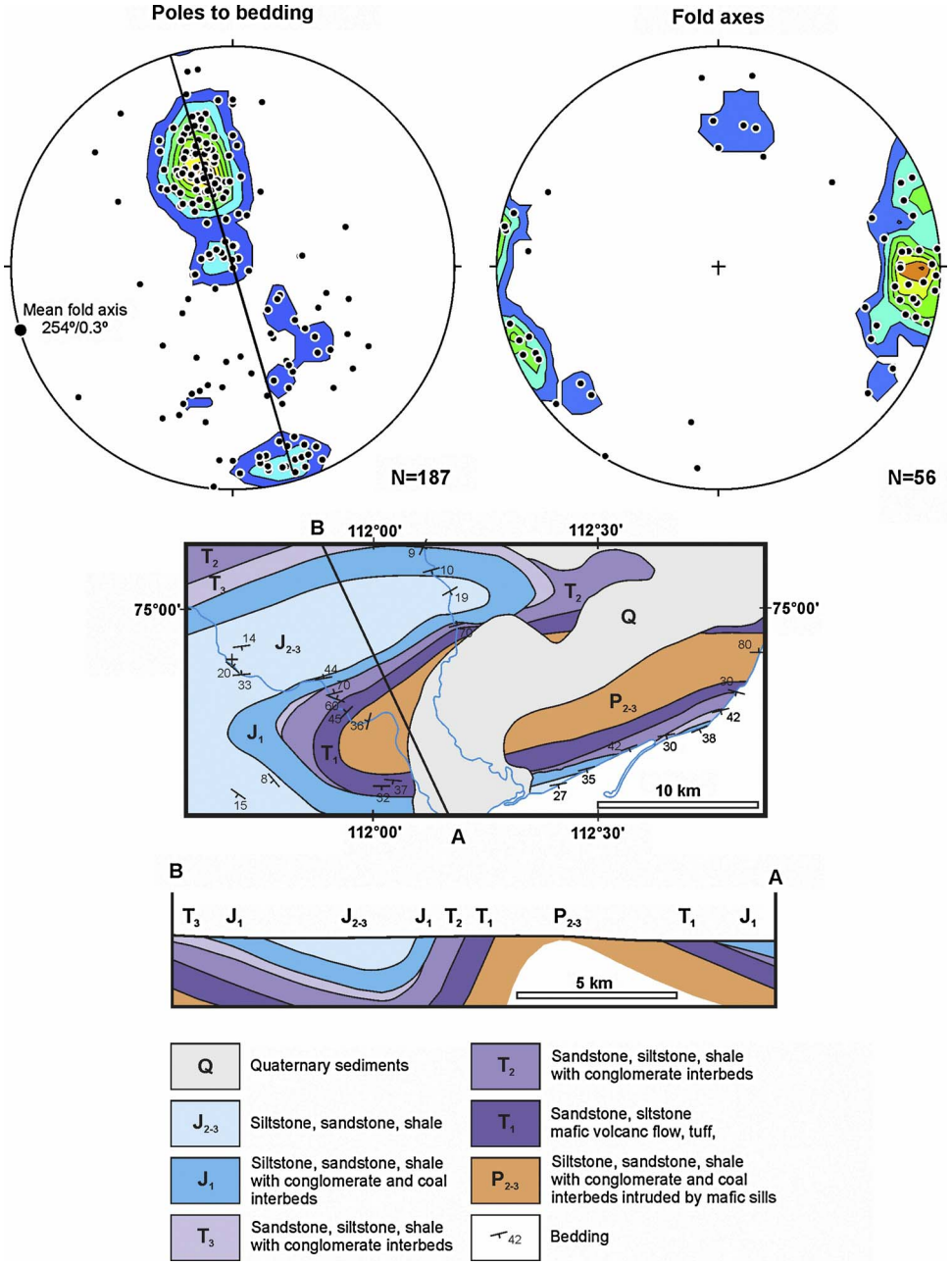

Fig. 7. Tsvetkova Cape key area. Poles to bedding and axes of minor folds are shown on Schmidt nets, lower hemisphere. Geologic map and cross-section compiled by Migai (1952) and modified by authors. Although pre-Jurassic angular unconformity is clearly recognized, Jurassic and older rocks are concordantly folded in NW-vergent folds. See Fig. 1 for location.

approximately 105° further east to 77° in the Anabar Bay area (Fig. 11) (Prokopiev and Deikunenko, 2001).

Small faults with slickensides have been documented throughout the study area. Only 1 out of 39 faults have predominant dip-slip displacement, the other 38 faults are strike-slip faults. Dextral and sinistral displacements are of equal distribution. No cross-cutting relationships between dextral and sinistral strike-slip faults have been documented. However, some of them form structures similar to conjugate faults that were formed in the same stress field and, therefore, we combine all faults together in one population to estimate the stress axes (Fig. 11). The average north-east trend of the compression axis is in reasonable agreement with sinistral displacement along the Olenek FZ as proposed by Prokopiev and Deikunenko, 2001.

4. Geochronological and thermochronological study: methods and results

To examine the cooling and exhumation history of the eastern TSZ, new U-Pb, Ar-Ar and AFT studies of 40 samples of magmatic, metamorphic and sedimentary rocks from the Northern, Central and Southern Taimyr domains have been performed. Most of the efforts were focused on the AFT dating of samples to constrain the timing of episodes of late Paleozoic – Mesozoic cooling, which could be tied to regional tectonic events. Location and rock types of samples are provided in Suppl. 1 and are shown in Fig. 1.

4.1. U-Pb zircon and Ar-Ar muscovite geochronology

4.1.1. U-Pb granite intrusion dating

Two granite samples (G-1 and G-2) have been dated using the

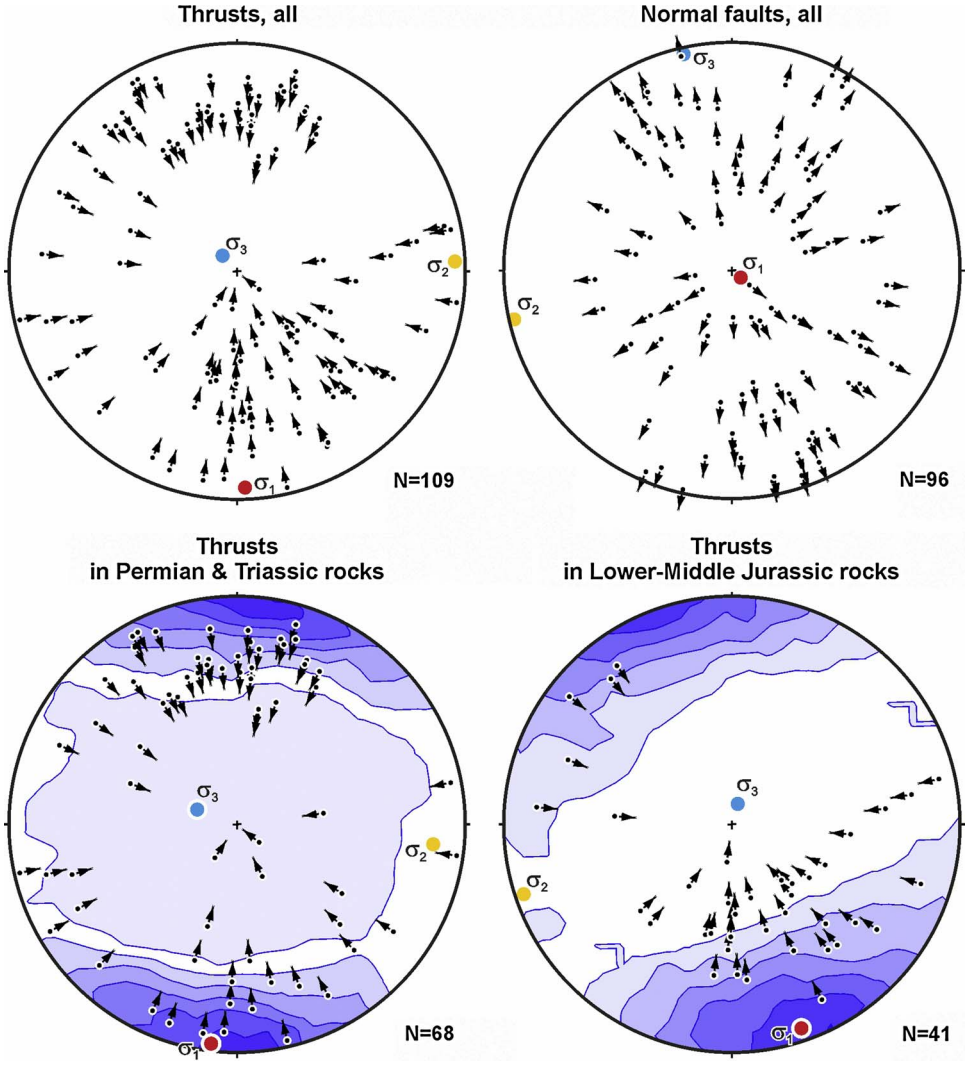

Fig. 8. Stress field restoration for the Tsvetkova Cape area based on study of small faults with slickenlines. N – number of measurements. Arrows show hanging wall slip direction inferred by slickenline orientation and predominantly calcite slickenfibers. Schmidt net, lower hemisphere. σ_1–axis of compression, σ_2–intermediate axis, σ_3–axis of tension. Stress axes were calculated using FaultKin software (Marrett and Allmendinger, 1990; Allmendinger et al., 2012). Note that compression and tension axes calculated for thrusts approximately parallel to tension and compression axes calculated for normal faults correspondently. Stress fields calculated for thrusts in Permian-Triassic rocks and Jurassic rocks are almost identical showing that although they are separated by angular unconformity (Fig. 7), they were deformed in the same stress field.

SHRIMP-II facilities at the All-Russia Geological Research Institute in St. Petersburg (VSEGEI). The analytical procedure, cathodoluminescence (CL) images and data are given in Suppl. 2 and 3, whereas concordia plots for each sample are illustrated in Fig. 12.

Sample G-1 is a hornblende-biotite granodiorite from the southern part of the intrusion that cuts Neoproterozoic and lower Paleozoic rocks in the northern part of the Central Taimyr Domain (Fig. 1). On recently published maps, this intrusion is shown as belonging to the Carboniferous – Early Permian magmatic complex (Makariev and Makarieva, 2011; Petrov, 2012). Zircon grains selected for dating are shown on CL images in Suppl. 3. Their euhedral shape, oscillatory zoning, and Th/U ratio varying from 0.65 to 2.06, suggest a magmatic origin. U-Pb dating of 10 grains yields a concordia age of 257 ± 4 Ma (Fig. 12a), in agreement with a whole-rock Rb-Sr isochron age of 258 ± 28 Ma,

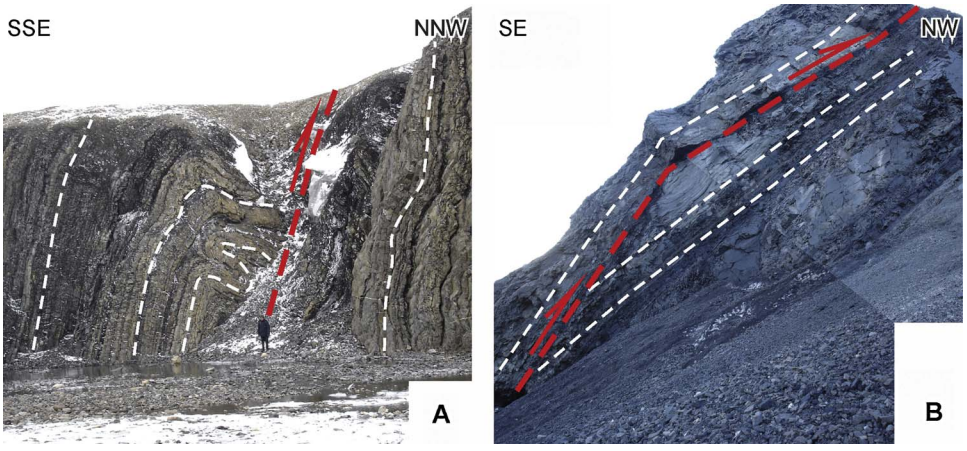

Fig. 9. NW-vergent thrusts in natural outcrops, Southern Taimyr Domain. A – Thrust with well-preserved flat-and-ramp geometry, Triassic rocks near Tsvetkova Cape. B – Thrust with hanging wall anticline, Cambrian rocks, Leningradskaya River. Both thrusts are parallel to bedding.

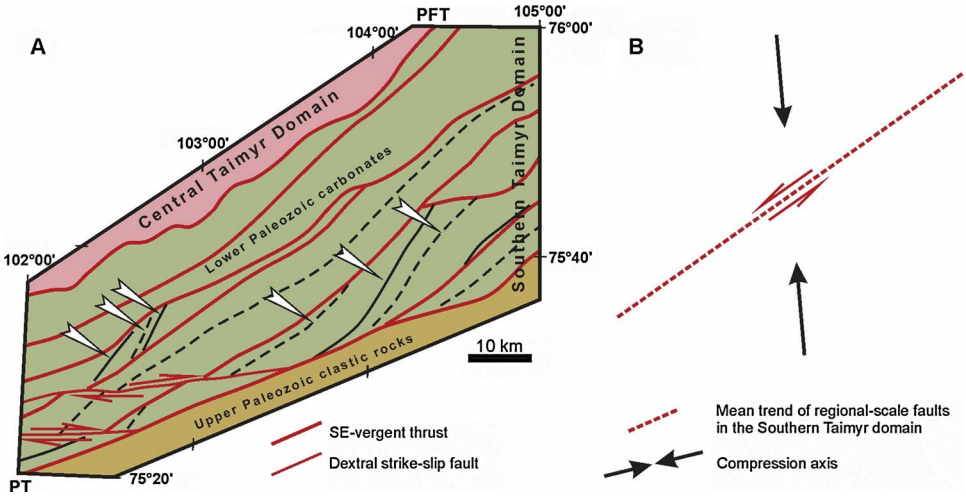

Fig. 10. Strike-slip faults with opposite sense of shearing along the major faults in the Central and Southern Taimyr domains. A – Structural map of central part of the Southern Taimyr Domain, data source Proskurnin (2009a). See Fig. 1 for location. Oblique relationship between axes of folds in en-echelon arrays marked by white arrows and trend of bounding thrusts is typical for shear zones with dextral displacement. E-W-trending dextral strike-slip faults were mapped in the south-east part of the study area. B – Relationship between trend of the major thrusts and compression axis estimated for the Svetliy Creek and Tsvetkova Cape areas (Figs. 4c, 8) supporting sinistral displacement along thrusts.

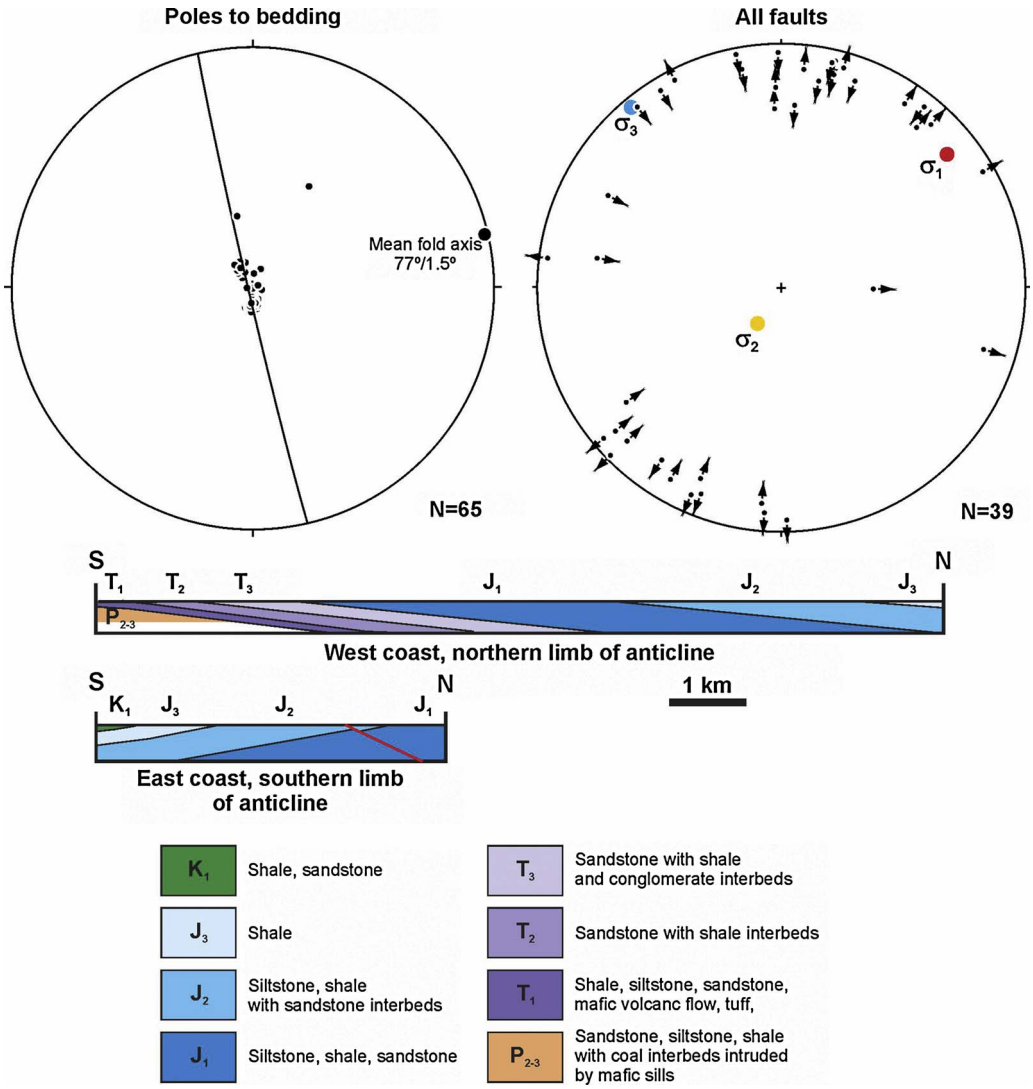

Fig. 11. Anabar Bay key area, cross-section via anticline representing the Olenek FZ (see Fig. 1 for location). Unconformity between Jurassic and underlying rocks does not affect the structural style and not recognized in cross-section. Stress field restoration is based on study of small faults with slickenlines. Strike-slip faults predominate. N – number of measurements. Arrows show hanging wall slip direction inferred by slickenline orientation and predominantly calcite slickenfibers. Schmidt net, lower hemisphere. σ_1–axis of compression, σ_2–intermediate axis, σ_3–axis of tension. Stress axes were calculated using FaultKin software (Marrett and Allmendinger, 1990; Allmendinger et al., 2012).

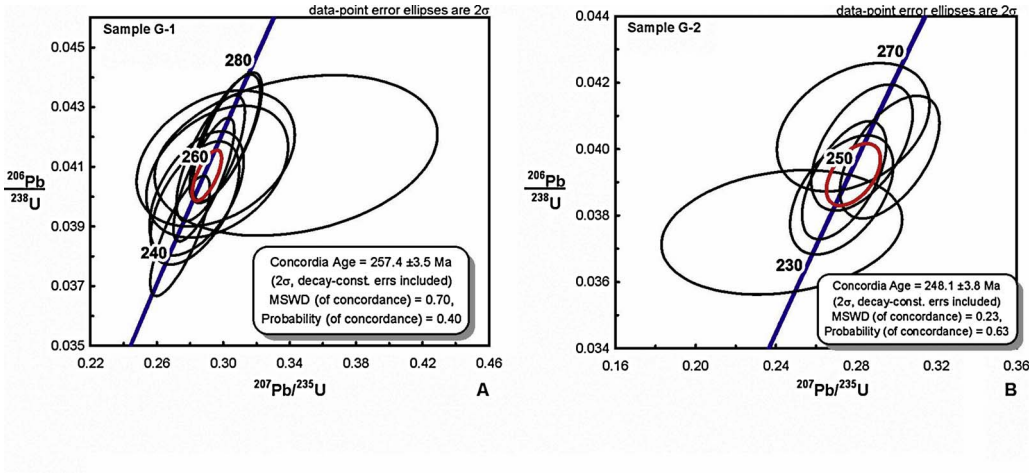

Fig. 12. Concordia plots for granite intrusions G-1 and G-2 (see Fig. 1 and Suppl. 1 for location).

estimated from a set of samples from adjoining granite intrusions (Vernikovsky et al., 1998).

Sample G-2 is from a granosyenite intrusion that cuts both lower Paleozoic rocks and the G-1 granodiorite intrusion. On, recently published maps, this intrusion is shown as belonging to the Late Permian magmatic complex (Makariev and Makarieva, 2011; Petrov, 2012). CL images of zircon grains selected for dating are shown in Suppl. 3. Their elongated euhedral shape, oscillatory zoning, and Th/U ratio varying from 0.65 to 3.47, again suggest a magmatic origin. However, zoned cores and uniform light-grey overgrowths have been identified in a few grains. Seven grains were dated, with one grain being dated in two spots, one in the core and one in the overgrowth. Six out of seven zircon grains yield a concordia age of 248 ± 4 Ma (Fig. 12b). One grain has a Neoproterozoic core and overgrowth that is slightly younger than the inferred concordia age, but has a very large reverse discordance. The new U-Pb age is a bit younger than ages proposed from previous studies by Vernikovsky et al. (1998) (252–264 Ma), but is still in reasonable agreement.

4.1.2. Ar-Ar metamorphic rocks dating

Our $^{40}Ar/^{39}Ar$ study of metamorphic muscovite from 3 samples was performed at the Rare Gas Geochronology Laboratory, University of Wisconsin-Madison, United States, using methods summarized by Smith et al. (2003) and Alexandre (2012). Data have been reduced and ages calculated using ArArCALC-software (Koppers, 2002). All original $^{40}Ar/^{39}Ar$ data are given in Suppl. 4–6 and the age spectra plots for each sample are illustrated in Fig. 13. All samples are from Neoproterozoic – lower Paleozoic rocks of the Central Taimyr Domain. According to Reiners et al. (2005), the closure temperature for the $^{40}Ar/^{39}Ar$ isotopic system in muscovite is estimated as 350°–300 °C.

Sample X-520 is a shale from the uppermost part of the Neoproterozoic Stanovskaya Fm, altered by low-grade metamorphism into slate with fine muscovite grains on the cleavage surface. The plateau age was calculated using 55% of ^{39}Ar released and is 266 ± 4 Ma (Fig. 13a, Suppl. 4). The age of the muscovite overlaps, within error, with age of the oldest granite intrusions (264 ± 8 Ma) from the post-collisional magmatic complex (Vernikovsky et al., 1998).

Sample X-542-4 is a phyllite from the central part of an approximately 15–20 m thick W-dipping bedding-parallel shear zone located within the Upper Cambrian shales. The plateau age was calculated using 76% of ^{39}Ar released and is 288 ± 4 Ma (Fig. 13b, Suppl. 5). The age corresponds with late stages of granite magmatism related to the Kara Terrane collision (Vernikovsky, 1996; Makariev, 2013).

Sample X-546-1 is a Mesoproterozoic mica schist interbedded with quartzite. A more detailed description of this unit (Oktyabr Fm) was published by Priyatkina et al. (2017). Mesoproterozoic rocks are thrust onto the Neoproterozoic Stanovskaya Fm along the fault zone, which represents the north-eastward continuation of the thrust mapped in the Svetliy Creek area (Fig. 4). An increasing metamorphic grade in the studied sample is likely related to closer proximity to the thrust surface. The plateau age was calculated using 89% of ^{39}Ar released and is 646 ± 2 Ma (Fig. 13c, Suppl. 6), slightly older than the late Neoproterozoic metamorphic event dated by Vernikovsky et al. (2004) at ca. 626-575 Ma.

4.2. Apatite fission track (AFT) low-temperature thermochronology

4.2.1. Basic approaches

AFT dating is often used in thermochronological studies, as the annealing (resetting) behavior of fission tracks in apatite is well understood to occur within the ~60–110 °C temperature interval, known as the partial annealing zone (PAZ) (O'Sullivan and Parrish, 1995; O'Sullivan et al., 1999; Lisker et al., 2009). Within the PAZ, fission tracks become progressively shorter and are eventually removed during thermal annealing. Since fission tracks initially form with a similar length of ~16 μm, the AFT length distribution is a sensitive monitor of the thermal history of the host rock and can be used to quantify the amount of annealing a sample has experienced (Gleadow et al., 1986; Green et al., 1989; Ketcham et al., 1999).

Thirty seven sandstone samples of variable metamorphic grade, and granite with ages varying from Neoproterozoic to Early Cretaceous, have been analyzed for AFT ages and confined track lengths at Apatite to Zircon Inc. following methods outlined by Donelick et al. (2005). A summary of the AFT method and detailed description of laboratory procedures along with radial plots and HeFTy models are provided in Suppl. 7.

Both the pooled age and central age for each sample were calculated; most pooled ages are based on 37–40 grains (Suppl. 8). The pooled AFT ages were calculated using the HeFTy modeling program (discussed below). RadialPlotter software by Vermeesch (2009) was used to calculate the central age. Although the U concentration is rarely used as a discriminator, a correlation between lower (younger) AFT age and high U concentration in individual grains has been reported (Glorie et al., 2017 and references therein). In all radial plots, single-grain AFT ages are color-coded according to their uranium concentration (in ppm) (Suppl. 7). For the central age calculation, a few grains with ages close to 0 Ma and older than 1500 Ma were filtered out. In two samples (82101 and KAM-2), only 6 grains were accepted for analysis, resulting in central ages with significant errors. For most samples, pooled and central ages are concordant and overlap within 1σ error. In two samples (M-73z and AA28P), the central age is significantly older than the pooled age as a result of the presence of a few old grains with precise

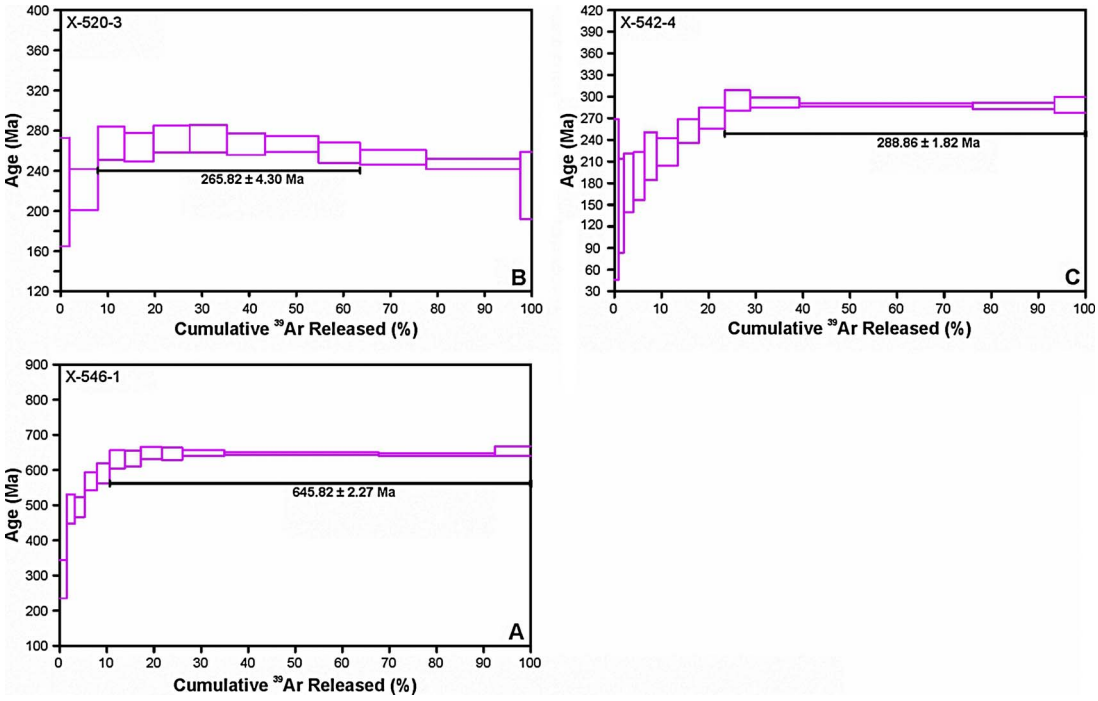

Fig. 13. $^{40}Ar/^{39}Ar$ age spectra for metamorphic muscovite from samples X-520-3, X-542-4, X-546-1 (see Fig. 1 and Suppl. 1 for location).

AFT ages. Except for ages associated with the HeFTy models, all ages referred to in the text and figures are central ages reported with 1σ error.

The χ^2 statistic test is used to detect the probability that all grains counted belong to a single population of ages. In 28 out of 37 samples, χ^2 of the central age is less than 5%, implying that multiple grain-age populations might be present. When multiple grain-age populations are supported by FT age distribution, the RadialPlotter software was used to estimate peak ages.

More than 100 tracks were typically used for the thermal history modeling, and only 2 samples (M-73z and 82102) contained less than 50 tracks (Suppl. 9). HeFTy software (Ketcham et al., 2000; Ketcham, 2005) was used to produce thermal history models for each of the analyzed samples. This program tests alternative time-temperature histories by statistically assessing the goodness of fit between AFT length distributions generated by kinetic modeling of AFT annealing and measured AFT length distributions. For 3 samples (M 09-27, M 09-28-2z, M 09-31-1z) no accessible time-temperature paths were produced; HeFTy models for other samples are given in Suppl. 7.

4.2.2. Results

Most AFT samples were collected from outcrops located along the coast or river banks at elevations of less than 300 m above sea level. Three samples (44102-IV, 44102-VII and 56147-X) are from shallow boreholes from depths less than 150 m. The low range in sample elevations means that topography should not have a significant impact on the thermal history of the samples. Moreover, previous studies by Zhang et al. (2018) concluded that there was no systematic relationship between AFT age and elevation.

A wide range in the mean track lengths and standard deviations, as well as low χ^2 values, suggest a predominance of samples with mixed ages (Suppl. 8, 9). Most studied samples are sedimentary rocks and two well-recognized geological processes lead to formation of mixed ages in such rocks: grains from multiple sources of clastic material, or differential annealing between grains of differing composition. Our interpretation of grains with mixed ages is based on approaches discussed by Gleadow et al. (1986); Green (1986); Fitzgerald and Gleadow (1988), O'Sullivan and Parrish (1995); O'Sullivan et al. (1999) and presented in Fig. 14.

The boomerang plot (Fig. 14a) shows the relationship between mean track length and AFT age for a set of samples that has undergone cooling from different paleotemperatures within and above (higher temperatures) the PAZ. Samples that have been cooled after one (older) heating event, and were affected by only low maximum temperatures during the second heating event, maintain the older original unreset age. Meanwhile, samples which were cooled after a second (younger) heating above ~110 °C, with total annealing during the second heating event, have been reset and display much younger fission track ages of the second event (fully reset ages). Both sets of original samples, including those unaffected by younger heating as well as and fully reset samples, have relatively long mean track lengths (Fig. 14a). Between these two end members, due to increasing influence of the second (younger) heating event, the mean track length first decreases as the partially annealed tracks are progressively shortened. Increased annealing of the older component decreases the number of tracks in it, causing the mean track length to start increasing once again towards the long mean track length characterizing the fully reset ages, whereas all pre-existing tracks are removed. The standard deviation follows the opposite trend, being lowest in grains with original unreset and fully reset ages, and highest in grains with low mean track length (Gleadow et al., 1986; Green, 1986). According to Gleadow et al. (1986), grains with fully reset ages have mean track lengths close to or greater than 14 μm and standard deviations ranging from 0.77 to 1.33 μm, with most between 0.8 and 1.0 μm. Fission track ages get progressively younger as temperature increases.

Fig. 14b shows the variation in the AFT age distribution for the same set of samples that were discussed in Fig. 14a. Samples that underwent cooling after only one (older) heating event have only one peak on the AFT age probability plot distribution corresponding to the older original unreset ages. Samples that experienced a second cooling event after exposure to paleotemperatures above ~110 °C also record only one peak on the AFT age probability plot distribution, related to the younger fully reset ages (Fig. 14b). Samples affected by the second cooling event after heating within the PAZ have a bimodal AFT age distribution, representing occurrence of grains with both older original unreset and younger fully reset ages. As the sample was progressively

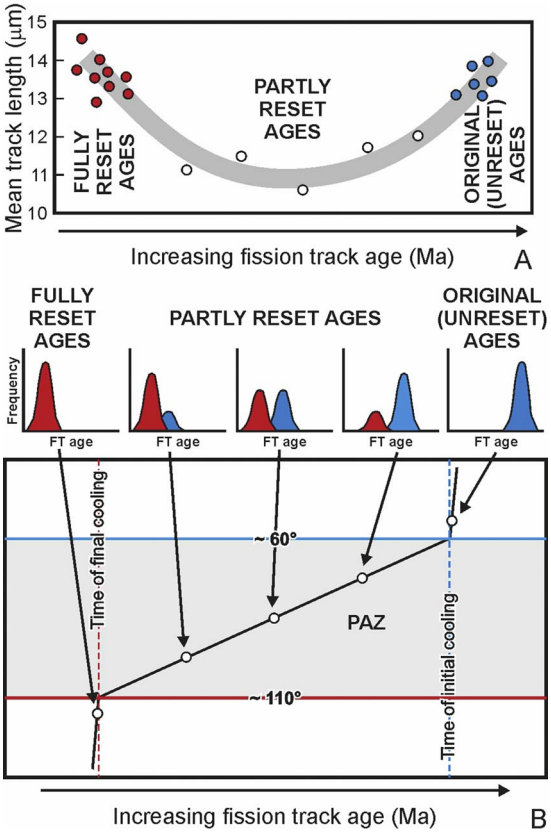

Fig. 14. Main approaches for AFT data interpretation. A – Boomerang plot showing relationship between mean track length and AFT age for a set of samples which was affected by two stages of heating and undergone cooling from different maximum paleotemperature at the same time (O'Sullivan and Parrish, 1995). Within the PAZ with increasing temperature AFT age decreases from samples affected by only one heating event (original unreset ages) to samples that passed through the PAZ (fully reset ages). In contrast to it, mean track length decreases due to heating of grains with unreset ages and then started to increase due to increasing number of reset grains. B – Relationship between AFT and temperature as PAZ was brought to surface by two events of rapid uplift. Diagrams in the upper part of the plot show proposed single-grain age distribution relative to a sample's position within the PAZ with gradual change in amount of old (blue) and young (red) ages from unreset to fully reset populations that occur outside the PAZ (after Fitzgerald and Gleadow, 1988, O'Sullivan and Parrish, 1995; O'Sullivan et al., 1999). See text for discussion. (For interpretation of the references to colour in this figure legend, the reader is referred to the web version of this article.)

heated, the number of younger reset ages increased, whereas the number of older original ages decreased. Younger grain ages forming the less abundant population in the bimodal age distributions are similar to the age of grains with fully reset ages and can be used to estimate the timing of the second cooling event. By contrast, grains with original ages were progressively heated in the PAZ and their partly reset ages are younger than the original ages.

Following the interpretations presented in Fig. 14, we now discuss the cooling history of samples presented in Suppl. 8, 9. Note, the actual mean track length and AFT age distributions might in reality be more complicated than presented in Fig. 14, since detrital apatite grains may come from multiple sources with different cooling histories and multiple original grain-age populations. Samples located in different tectonic structures are shown by different colors and are interpreted separately (Figs. 1, 15). In comparison with the original data set presented in Suppl. 8, 9, we exclude from the following discussion KAM-2 and 82102 samples, as their central age was calculated using only 6 grains, and M 73z and AA28P samples, which have very different central and pooled ages.

Data from samples from the Northern and Central Taimyr domains plot along a boomerang-like trend, with the majority of data points supporting an upward trend of mean track length, suggesting resetting of the original ages (Fig. 15). Sample 102-4 of Cambrian quartzite is the only data point that likely retains mostly original unreset AFT grain ages. Its AFT age of 312 ± 15 Ma is similar to that of recorded timing of granite magmatism widely distributed in the Northern and Central Taimyr domains (Vernikovsky, 1996; Makariev, 2013; Kurapov et al., 2018). The sample has a reasonably high mean track value (13.68 μm) and low standard deviation (1.31 μm) (Suppl. 9), which are similar to those described by Gleadow et al. (1986) as being unaffected by significant subsequent heating. A lack of significant heating after rapid cooling at ca. 320-290 Ma is supported by HeFTy modeling (Suppl. 7). Sample 2670 with the lowest mean track value (13.01 μm) and relatively higher standard deviation (1.44 μm) displays a bimodal distribution of ages with peaks at 230 ± 19 Ma and 348 ± 45 Ma, although the distribution of high-uranium grains suggests that the youngest population calculated by RadialPlotter should actually be younger (Fig. 16). AFT ages of samples 957-59 and 625-6 are younger, along with a greater mean track length. HeFTy modeling suggests some reheating for samples 2670 and 957-59, but almost no reheating for sample 625-6, which produced the youngest AFT age and longest mean track length value. Five samples (44102-IV, G-1, G-2, A-2006-5, 56147-X) form an array with similar AFT ages and mean track length values ranging between 13.76 μm and 14.06 μm, which suggests these samples contain fully reset ages. Two granite samples from this array (G-1 and G-2) also have quite low standard deviations close to 1.3 μm. The other three samples were collected from poorly lithified sedimentary rocks where detrital apatite reflects thermal evolution of their provenance, but their standard deviations are also very low and close to 1.0 μm. HeFTy modeling also suggests very rapid cooling for samples G-1 and G-2, and a more complicated history for samples 44102-IV, A-2006-5, and 56147-X, with younger heating and cooling events. Therefore we infer AFT ages from G-1 and G-2 samples as the best estimation of the timing of a younger cooling event that affected a significant part of the Northern and Central Taimyr domains (Suppl. 8). The weighted mean age of G-1 and G-2 samples is 192 ± 11 Ma, slightly older than the weighted mean age of all five samples of 187 ± 7 Ma (2σ) (Fig. 17a).

Samples from the Southern Taimyr Domain, Olenek FZ and Yenisey-Khatanga Depression form another boomerang-like distribution (Fig. 15). As all these samples are sedimentary rocks, interpretation of the results is more complicated. Samples M 09/31-1z, HUD-5, M 09/28, M 09/34z and M 09/32z plot along a trend with similar ages and mean track lengths, which vary between 13.8 μm and 14.02 μm, with standard deviation between 1.27 μm and 1.42 μm. HeFTy modeling of these data suggest rapid cooling for the HUD-5 sample and more complicated histories for the M 09/32z and M 09/34z samples, although they are unlikely to have been exposed to elevated paleotemperatures after cooling (Suppl. 7). These samples dislay the youngest ages in the sample set, so we interpret them as the fully reset ages with a weighted mean age of 120 ± 6 Ma (Fig. 17b). Data from other samples plotted along the same trend (Fig. 15), but with shorter mean track lengths (TT-27-1La and TT-64zx samples), produced a bimodal distribution of AFT ages with peaks estimated by RadialPlotter as 117 ± 10 Ma and 199 ± 9 Ma for TT-27-1La, and 146 ± 8 Ma and 231 ± 14 Ma for TT-64zx (Fig. 16). However, distribution of the grain ages from TT-27-1La indicates that there are grains significantly younger than 146 ± 8 Ma, and that the actual heating event is likely to be either younger than that based on the grain-age population as calculated by RadialPlotter, or suggest the existence of an even younger event not yet recognized in any of the other data points. HeFTy modeling suggests that exposure of these samples to elevated paleotemperatures after sediment deposition was quite likely (Suppl. 7). In comparison with the TT-27-1La and TT-64zx samples, data from samples M 09/27 and M 09/35z reveal younger AFT ages and longer mean track lengths, which form an upward trend of mean track length at ~120 Ma (120 ± 6 Ma population of grains with fully reset ages) (Fig. 15). The only sample with an original unreset age might be M-52, with a high mean track length

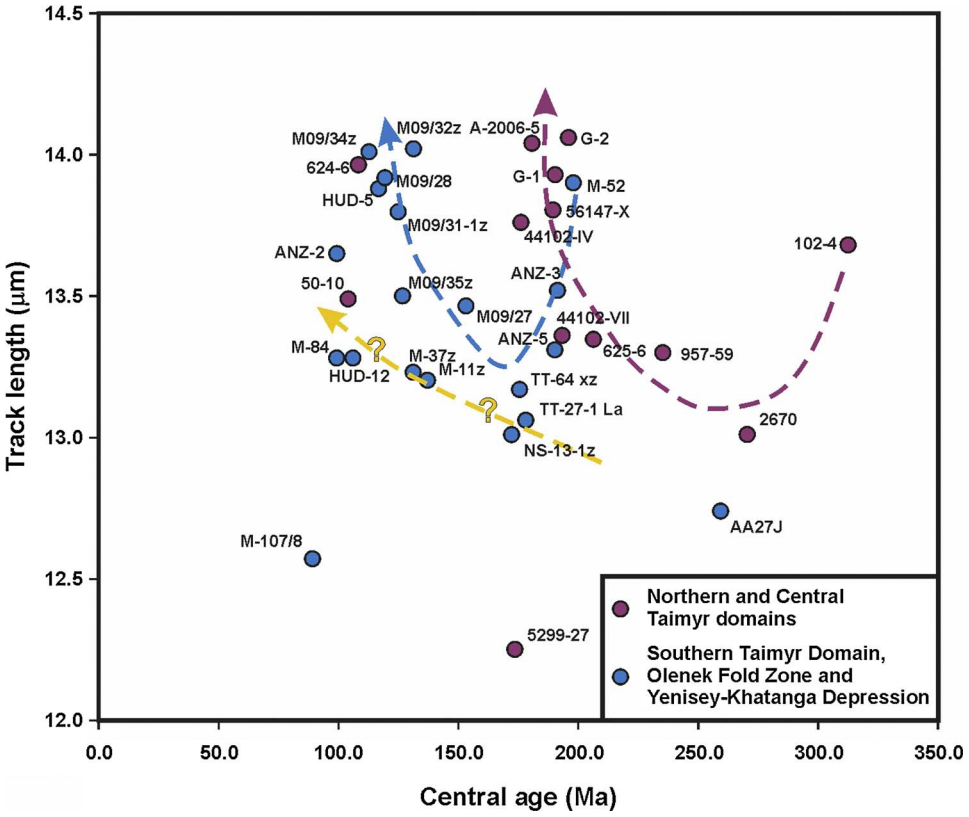

Fig. 15. The mean track length vs central age diagram for samples from different tectonic structures (see Fig. 1 and Suppl. 1 for location). Magenta line – boomerang-like trend for samples from the Northern and Central Taimyr domains started at ca. 312 ± 15 Ma (sample 102-4) original unreset age and continued up to ca. 187 ± 7 Ma fully reset ages, blue line – boomerang-like upward trend for samples from the Southern Taimyr Domain, Olenek Fold Zone and Yenisey-Khatanga Depression continuing to ca. 120 ± 6 Ma fully reset ages. Yellow line with question marks – proposed part of boomerang-like upward trend for samples affected by a younger (ca. 100-80 Ma) cooling event. (For interpretation of the references to colour in this figure legend, the reader is referred to the web version of this article.)

(13.9 μm) and moderately low standard deviation (1.5 μm). The M-52 sample belongs to the same array as samples from the Northern and Central Taimyr domains, with fully reset ages at 192 ± 11 Ma. The central age of the M-52 sample is 198 ± 9 Ma, which overlaps within error with 192 ± 11 Ma, indicating that they are likely to be from the same population. Meanwhile, samples from the Southern Taimyr Domain, Olenek FZ and Yenisey-Khatanga Depression form another complete boomerang plot with an initial cooling event of the same age as the final cooling event in the Northern and Central Taimyr domains (Fig. 15).

A third cooling event is suggested by closely located samples N-13-1z, M-11z, M-37z, and M-84 from the Tsvetkova Cape area and further to the south (Fig. 1). The stratigraphic ages of these samples vary from Permian to Early Cretaceous and they follow an upward trend of mean track length (Fig. 15). The age of the youngest peak estimated by the RadialPlotter software varies between ca. 100 Ma and 60 Ma indicating a Late Cretaceous cooling event (Fig. 16). All these samples have only partially reset ages, suggesting that none of them passed through the PAZ and were heated above 110 °C.

The M-107/8 and 5299-27 samples have a low mean track length and are quite distinct from the discussed trends outlined in Fig. 15. We interpret these results as a consequence of a complicated thermal history of these samples, which were pushed into the PAZ several times but were never fully annealed.

5. Discussion

5.1. Structural style: thin-skin vs thick-skin tectonics

Structural style of the Southern Taimyr Domain has been interpreted in two different ways. Inger et al. (1999) interpreted the structure as thin-skinned tectonics, where the present-day steep dip of the fault planes was interpreted as a result of their subsequent rotation during younger deformation events. On the other hand, Pogrebitsky and Shanurenko (1998) and Vernikovsky and Vernikovskaya (2001) proposed the predominance of basement-involved tectonics in the Southern Taimyr Domain. Zhang et al. (2018) also suggest that only basement-involved thick-skinned tectonics occurred throughout the Central and Southern Taimyr domains.

Our observations favor the thin-skinned tectonic interpretation of the Southern Taimyr Domain structure. Bedding-parallel thrusts, shown in Fig. 5, are widely distributed in the Southern Taimyr Domain and are characteristic of thin-skinned rather than thick-skinned tectonics. Based on maps by Bezzubtsev et al. (1983), Proskurnin (2009a) and Proskurnin et al. (2016), a sequence of thrust-bounded blocks with repeating structure and stratigraphy are found within the Southern Taimyr Domain to the north-west of the Pogranichniy Thrust. They are composed of Ordovician to Lower Permian rocks and contain a hanging wall anticline and/or a footwall syncline, partly truncated by the bounding thrust. The geometry of the bounding thrusts is similar to that shown in Fig. 5. This repetition of stratigraphy and structure is typical for stacked thin-skinned imbricate thrust sheets but not deeper basement-involved tectonics. The areas with a predominance of upper Paleozoic – Triassic clastic rocks have a more complicated structural style, but the occurrence of fault-bounded zones with similar stratigraphy, structure and predominantly SE-vergent folds further support the interpretation by Inger et al. (1999). In summary, our compilation of available data from structural studies and geological maps of variable scales would favor interpretation of the Southern Taimyr Domain as a thin-skinned fold and thrust belt.

A cross-section through the Southern Taimyr Domain and much of the Central Taimyr Domain based on the thin-skinned tectonic model is presented in Fig. 18. The oldest rocks identified within the thrust sheets are of Lower Ordovician age, suggesting that the basal detachment is likely to be located within Lower Ordovician or Upper Cambrian rocks, and that the Ediacaran – Lower Cambrian rock unit along with underlying basement are likely to be autochthonous. To the south-east of the Pogranichniy Thrust, the oldest rocks exposed in cores of anticlines are usually Middle Carboniferous – Lower Permian clastic rocks forming the lowermost unit in the clastic succession, suggesting that the

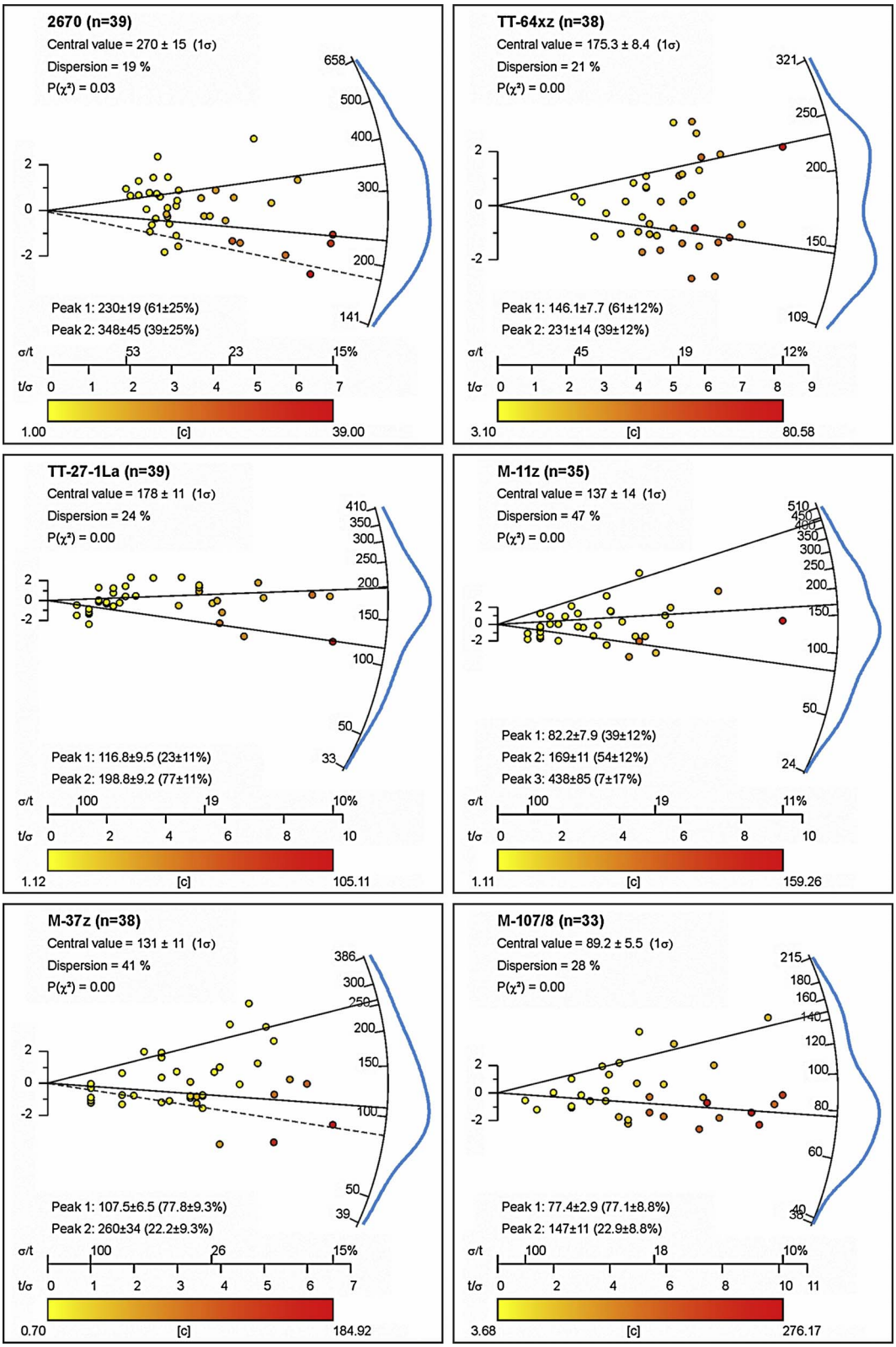

Fig. 16. Representative radial plots for samples cooled after heating within PAZ. Color bar shows concentration of uranium. Blue line is AFT age distribution produced by RadialPlotter. n – number of grains involved in radial plot. Sample 2670 (Northern Taimyr Domain, magenta trend in Fig. 15) shows bimodal AFT ages distribution. However, a trend following most precise youngest grains with the highest uranium concentration implies a cooling event at approximately 190-180 Ma (dashed line). Samples TT-64zx, TT-27-1La, M-11z and M-37z are from the Tsvetkova Cape area of the Southern Taimyr Domain (blue and yellow trends in Fig. 15) and show bimodal or more complicated AFT age distribution with the latest cooling event much younger than ca. 190-180 Ma event recorded for sample 2670. Although the youngest peak age for sample M-37z is 108 ± 7Ma, a trend following most precise youngest grains with the highest uranium concentration implies a younger cooling event. Sample M-107/8 is from Yenisey-Khatanga Depression outside any trends (Fig. 15), but also show evidence for a young ca. 77 ± 3 Ma event. (For interpretation of the references to colour in this figure legend, the reader is referred to the web version of this article.)

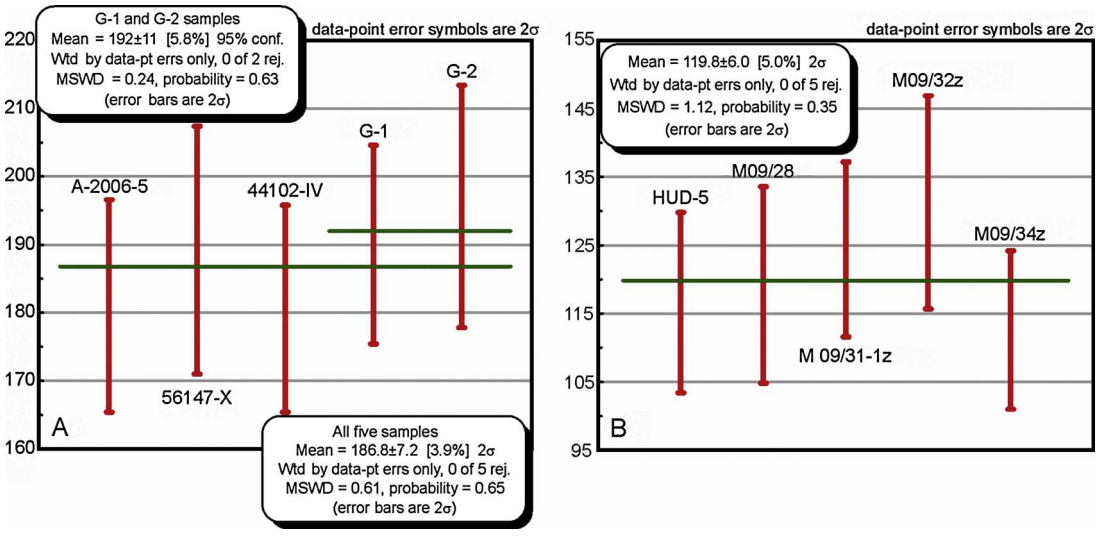

Fig. 17. Weighted average values for fully reset ages from Northern and Central Taimyr Domain (A) and Yenisey-Khatanga Depression including Olenek Fold Zone and Southern Taimyr Domain.

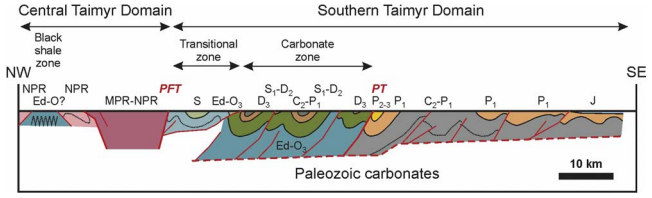

Fig. 18. Cross-section showing structural styles of the Central and Southern Taimyr domains (no vertical exaggeration).
Data Source: Proskurnin (2009a), Proskurnin et al. (2016), Makariev and Makarieva (2011) and observations by authors. Ed – Ediacaran. PFT – Pyasino-Faddey Thrust, PT – Pogranichniy Thrust.

basal detachment here separates an allochthonous upper Paleozoic – Triassic succession from autochthonous or para-autochthonous lower Paleozoic carbonates. Although the intensity of deformation decreases south-eastward, the base-Jurassic unconformity can be clearly recognized on geological maps (Pogrebitsky, 1998; Proskurnin 2009a; Proskurnin et al., 2016).

The origin of NW-vergent thrusts similar to those mapped in the Svetliy Creek area (Fig. 4) and shown in the north-western part of the cross-section is ambiguous (Fig. 18). They might represent a positive flower structure formed during dextral strike-slip displacement and related transpression. Alternatively, these thrusts might be synchronous with other NW-vergent thrusts and folds documented throughout the Southern Taimyr Domain (Figs. 7, 9), suggesting that related tectonic events had a very widespread distribution.

5.2. Late Paleozoic tectonic event

The Carboniferous – Early Permian collision between the Kara Terrane and the Siberian Craton is traditionally proposed as the main tectonic event responsible for formation of TSZ (Vernikovsky, 1996; Vernikovsky et al., 2004). Although our new U-Pb results suggest that ca. 250 Ma post-collisional granite intrusions are more widespread than those shown on geological maps, numerous Early Carboniferous – Late Permian (ca. 345-268 Ma) granite intrusions in the Northern Taimyr Domain provide important evidence of the late Paleozoic active margin and collisional processes (Vernikovsky et al., 1998; Makariev, 2013; Kurapov et al., 2018).

However, samples that retain AFT evidence of the late Paleozoic deformations are reported from only the Northern Taimyr Domain, namely from the Severnaya Zemlya archipelago (Figs. 1, 15). Most of the tectonic structures formed during the late Paleozoic were overprinted by subsequent Mesozoic tectonic events and are difficult to recognize in the present structural framework. New Ar-Ar dating of metamorphic muscovite at 266 ± 4 Ma and 288 ± 4 Ma support the occurrence of Permian tectonic events, but one of the samples retained Neoproterozoic muscovite (646 ± 2 Ma) (Fig. 13). This sample suggests that there are discrete areas within the Central Taimyr Domain where the Ar-Ar isotopic system was not reset since the Neoproterozoic, and which were consequently much less affected by deformation and metamorphism during the Carboniferous – Permian tectonic event. Furthermore, the absence of unconformities within the Paleozoic-Triassic succession is also problematic for the interpretation of the late Paleozoic deformation events in the Southern Taimyr Domain. Within the Severnaya Zemlya archipelago, late Paleozoic folds and thrusts have been documented, but they have a limited distribution. Most of the archipelago contains a sedimentary cover of gently-dipping Ordovician and younger rocks which, according to U-Th/He zircon dating, have a maximum burial of < 7 km (Lorenz et al., 2007, 2008; Makariev and Makarieva, 2011; Ershova et al., 2015b, 2016b, 2018). The intensive late Paleozoic deformations must therefore have been restricted to a relatively narrow zone along the south-east margin of the Kara Terrane and adjacent parts of the Central Taimyr Domain, favouring an oblique style of collision with predominantly strike-slip displacement. Absence of late Paleozoic ophiolites and other relics of the oceanic crust further support juxtaposition of the Kara Terrane and Siberian Craton by strike-slip displacement rather than subduction and closure of an ancient oceanic basin.

Recent provenance and geophysical studies favor close affinity of the Kara Terrane with the Timanides along the northeast margin of the East European Craton (Gee et al., 2006; Lorenz et al., 2008; Ershova et al., 2016a, 2018 and references therein). Numerous 345-330 Ma detrital zircon grains in similarly aged clastic sediments in the northern Verkhoyansk FTB suggest that the most likely provenance areas for them were located within the Kara Terrane indicating that the timing of collision between Kara and Siberia occurred during the Late Visean (Ershova et al., 2015a). Although the main collisional phase in the Uralian Orogen has been dated as Middle Carboniferous (Late Bashkirian) – Permian, the onset of collision was diachronous and locally started in the Visean (Puchkov, 2009, 2010), corresponding well with our data on collision between Kara and Siberia. However, we still do not have convincing evidence as to wheather the studied late Paleozoic tectonic event was the beginning of an oblique collision between the East European and Siberian cratons, or if the Kara Terrane was

displaced from its initial location on the north-east margin of the East European Craton and moved towards the northern margin of the Siberian Craton along a strike-slip fault, in a similar way to that proposed by Metelkin et al. (2005, 2012).

5.3. Mesozoic tectonic events

Different authors estimated the timing of Mesozoic tectonic events and their relationship with the late Paleozoic event in different ways. According to Vernikovsky (1996) and Pogrebitsky and Shanurenko (1998), the main compressional event started in the Permian, was briefly interrupted by Early Triassic rifting in the Yenisey-Khatanga Depression, before continuing until the end of the Triassic. Similarly, Inger et al. (1999) argued for several stages of deformation including Early Permian, Late Triassic and late Mesozoic-Cenozoic. In contrast, Zonenshain et al. (1990) and Uflyand et al. (1991) suggested an Early Cretaceous age for the main deformation event. Drachev (2011) discussed 2 main orogenic events – in the Permian and close to the Triassic-Jurassic boundary. Pease (2011) suggested Late Triassic-earliest Jurassic and Early Cretaceous events, whereas Zhang et al. (2018) discussed several stages starting in the Early Permian and terminating in the Late Triassic.

To understand the Mesozoic tectonic history, we have focused our study on the key areas where the relationship between different tectonic structures and the AFT data can be observed. In the Podkhrebetnaya River area (Fig. 5), Ordovician to Lower Permian rocks are conformably folded to form a regional-scale syncline. Thrusts in the NW part of the area cut the NW limb of the syncline, showing that the main deformation stage occurred post-Early Permian. In the Tsvetkova Cape area, Permian and Triassic rocks are conformably folded with Triassic beds dipping 70° north-westward (Fig. 7). The main deformation event forming the modern structural style of the Southern Taimyr Domain must therefore have occurred after deposition of Triassic rocks in the Tsvetkova Cape area.

More structural studies are necessary to refine the details of the structural evolution of the TSZ. The angular unconformity at the base of the Jurassic is easily recognized on maps of different scales throughout the TSZ (Pogrebitsky, 1998; Proskurnin, 2009a; Proskurnin et al., 2016; Makariev and Makarieva, 2011), further supporting the occurrence of a tectonic event before deposition of Jurassic rocks. However, the uppermost Triassic rocks (uppermost Norian and Rhaetian) and, likely, lowermost Jurassic rocks (lower Hettangian) are missing in the most complete successions, giving an approximate age range of the tectonic event as latest Triassic – earliest Jurassic (Dagys and Kazakov, 1984; Pogrebitsky and Shanurenko, 1998; Nikitenko et al., 2013). This is in reasonable agreement with our AFT-based estimation of the cooling event of 192 ± 11 Ma documented throughout the Northern and Central Taimyr Domains (Fig. 15) showing that the latest Triassic – earliest Jurassic tectonic event affected the entire continental part of the TSZ. The intensity of the latest Triassic – earliest Jurassic tectonic event decreases northward, but it is still recognized in the Severnaya Zemlya archipelago (Ershova et al., 2015b).

The latest Triassic – earliest Jurassic tectonic event contained three deformation stages. The bedding-parallel outcrop-scale NW-vergent thrusts were formed before the main deformation stage and were subsequently rotated along with the host rocks (Fig. 9). Thus, the outcrop-scale NW-vergent thrusts represent the earliest deformation stage (D1). During the main deformation stage (D2), the modern structure with predominance of SE-vergent thrusts and folds similar to those in the Podkhrebetnaya River area (Fig. 5) was formed. The en-echelon array of map-scale folds (Fig. 10) is bounded by the D2 thrusts, and so their formation is likely to be related to the main deformation stage as well. Geometry of the en-echelon array of folds is typical for shear zones with dextral displacement, supporting the hypothesis that thrusts had a dextral component of displacement as discussed earlier (Bezzubtsev et al., 1986; Vernikovsky 1996; Makariev and Makarieva, 2011). A generation of dextral strike-slip faults cut NE-trending folds and faults, suggesting formation during a younger (D3) deformation stage. Triassic rocks are involved in the deformation and are unconformably overlain by Lower Jurassic rocks, confirming that the D1-D3 deformation stages all correspond to the latest Triassic – earliest Jurassic tectonic event.

NW-vergent folds in the Tsvetkova Cape area (Fig. 7) incorporate Jurassic rocks and are related to a post-Jurassic (D4) deformation event. This folding may be related to a transpression event (Inger et al., 1999), or, alternatively, to formation of blind back thrusts, which are typical for buried thrust fronts (e.g. Morley, 1986; Jones, 1996). The stress field documented in Jurassic rocks of the Tsvetkova Cape area is very similar to that documented far to the north-west in the Svetliy Creek area, suggesting that the post-Jurassic tectonic event was widely distributed, although likely to have been less extensive than the latest Triassic – earliest Jurassic event. According to our interpretation (Fig. 10b), the post-Jurassic stress field would be expected to induce sinistral displacement along major thrusts. Most AFT samples from the Tsvetkova Cape area follow a trend related to a ca. 100-60 Ma cooling event (Fig. 15), which we interpret as an estimation for the age of the D4 deformational event. The final deformation stage (D5) involved reactivation of thrusts as normal faults, and is documented in both the Central and Southern Taimyr domains (Figs. 4c, 8). The D5 deformation event is younger than the D4 event and is likely to be Cenozoic in age. However, the D5 event is not reflected in our AFT data making precise age determination more ambiguous.

No Mesozoic events resulted in complete resetting of AFT ages, complicating the interpretation of Mesozoic tectonic events in the Southern Taimyr Domain. Partial annealing is recognized in all samples, varying in age from Middle-Late Permian to Middle-Late Jurassic (samples M-11z, M-37z, TT-27-1La, TT-64xz, see Fig. 16 and Suppl. 7). Jurassic samples M-11z and TT-27-1La likely record a pre-Jurassic cooling in their provenance, and a later partial resetting by younger events at ca. 120 ± 6 Ma or ca. 100-60 Ma (Fig. 16). Cooling at ca. 100 Ma or later is recorded by Permian sample M-37z as well. Cretaceous deformations reported in the Southern Taimyr Domain are likely related to either the ca. 120 ± 6 Ma or ca. 100-60 Ma events. However, no Cretaceous rocks of Aptian age and younger are exposed close to the studied areas of the Southern Taimyr Domain, therefore AFT ages for Cretaceous cooling do not have any stratigraphic control.

In the Olenek FZ, both Jurassic and Triassic rocks have been folded, suggesting a post-Jurassic age of deformation (Fig. 11). However, both the structural style, with very gentle folding, and specific stress field typical for strike-slip environments, are very different from those in the Southern Taimyr Domain. Samples from the Olenek FZ (ANZ-2, ANZ-3, and ANZ-5) basically follow downward and upward trends on the boomerang plot, with fully reset ages close to 120 ± 6 Ma, but display only partial annealing (Fig. 15). However, in the Yenisey-Khatanga Depression to the south, the 120 ± 6 Ma cooling event predominates, resulting in complete resetting of AFT ages. In two Lower Cretaceous (Hauterivian-Barremian) samples (M 09/32z and M 09/34z), AFT ages were fully reset almost immediately after deposition.

Our structural and thermochronological studies highlight the widespread distribution of previously underestimated latest Triassic – earliest Jurassic and Cretaceous tectonic events, although their importance was pointed out by Verzhbitsky and Khudoley (2010) and Drachev (2011, 2016). It brings to the fore old ideas by Zonenshain et al. (1990) regarding predominantly late Mesozoic tectonics on the Taimyr Peninsula, although their interpretation of the Pyasino-Faddey Thrust as a suture formed during closure of the Anyui Paleocean seems to be incorrect (e.g. Drachev et al., 1998; Franke et al., 2008). However, latest Triassic – earliest Jurassic deformation in the Northern and Central Taimyr domains is similar in age to the main tectonic event in the Pai-Khoi – Novaya Zemlya Fold and Thrust Belt (Pai-Khoi – Novaya Zemlya FTB) (Lopatin et al., 2001; Korago and Timofeeva, 2005; Drachev, 2016; Prokopiev et al., 2016), lending strong evidence for a direct link between the Taimyr-Severnaya Zemlya and Pai-Khoi-Novaya

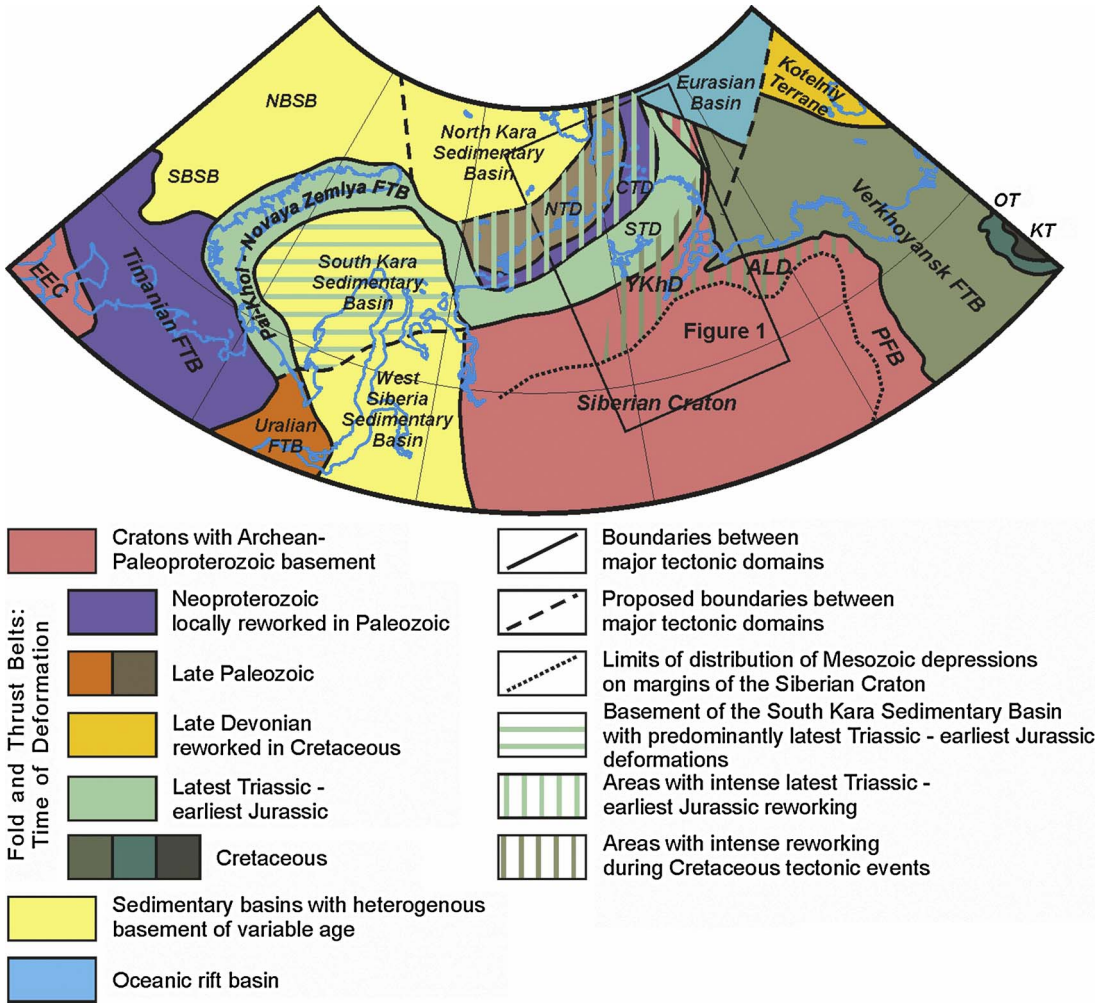

Fig. 19. Simplified tectonic map of the northern part of Siberian Craton and surrounding fold and thrust belts (after Drachev, 2016, modified). Note wide belt with predominance of Mesozoic (latest Triassic – earliest Jurassic and Cretaceous) framing the Siberian Craton. EEC – East European Craton, SBSB – South Barents sedimentary Basin, NBSB –North Barents Sedimentary Basin, NTD – Northern Taimyr Domain, CTD – Central taimyr Domain, STD – South Taimyr Domain, YKhD – Yenisey-Khatanga Depression, ALD – Anabar-Lena Depression, PFB – Priverkhoyansk Foreland Basin, OM – Omulevka Terrane, KT – Kolyma-Omolon Terrane.

Zemlya fold and thrust belts.

Our data on the almost synchronous beginning of the late Paleozoic collision in the Uralian Orogen and TSZ favor a direct link between them. If so, the most reasonable interpretation for the deformation of the Pai-Khoi-Novaya Zemlya FTB seems to be the embayment model proposed by Drachev et al. (2010) and Scott et al. (2010). The important part of this model is the presence of an embayment containing trapped oceanic crust (the present day South Kara sedimentary basin) along the margin of Baltica during the Paleozoic, followed by pushing of the West Siberia basement blocks into this embayment to form the Late Triassic – Early Jurassic Pai-Khoi-Novaya Zemlya FTB. This model explains why the Pai-Khoi-Novaya Zemlya FTB does not contain evidence of the late Paleozoic deformations documented to the east (TSZ) and south (the Urals), and is supported by recent structural studies (Curtis et al., 2018).

Possible correlatives of the two younger events at ca. 120 ± 6 Ma and 100-60 Ma are less obvious. Both events are quite close in age to High Arctic Large Igneous Province (HALIP) (e.g. Corfu et al., 2013; Estrada and Henjes-Kunst, 2013; Evenchick et al., 2015), but direct correlation of tectonic events in the amagmatic Southern Taimyr Domain and Yenisey-Khatanga Depression with HALIP seems to be unlikely. Magmatic and tectonic events of a similar age were reported from the Verkhoyansk FTB (e.g. Prokopiev and Deikunenko, 2001; Khudoley and Prokopiev, 2007), therefore correlation of tectonic events in the Olenek FZ, representing a western branch of the Verkhoyansk FTB, with those in the Verkhoyansk FTB seems to be most reasonable. A long-term complicated interplay of the TSZ with the Pai-Khoi – Novaya Zemlya FTB to the west, and the Verkhoyansk FTB to the east, resulted in a set of dextral and sinistral displacements along the main thrusts documented throughout the Central and Southern Taimyr domains as well as in the western termination of the Olenek FZ.

Our new data, combined with previous studies focused on the age of deformations in the Pai-Khoi – Novaya Zemlya and Verkhoyansk fold and thrust belts, show that areas affected by latest Triassic – earliest Jurassic and Cretaceous deformations form a wide belt framing the Siberian Craton, across its north-western, northern and eastern margins (Fig. 19). In its northern part, the intensity and age of deformations progressively decrease towards the Siberian Craton, as well as towards internal parts of the Kara Terrane. However, more studies are necessary to understand the origin of late Mesozoic deformations and their relationship with plate kinematics.

Finally, the widespread distribution of samples with fully reset ages within the eastern part of the Yenisey-Khatanga Depression (samples M 09/28, M 09/31-1z, M 09/32z, M 09/34z, see Figs. 1, 16) suggests that they were heated above 110 °C. The cooling event, related to an uplift and erosion phase, occurred at ca. 120 ± 6 Ma, when approximately 3–4 km of sediment was removed. The two youngest samples (M 09/32z, M 09/34z) are Hauterivian to Barremian (Early Cretaceous) in age

and only slightly older than the ca. 120 ± 6 Ma cooling event, suggesting rapid uplift and erosion. Therefore, we interpret the decreasing thickness of Cretaceous clastics eastward across the eastern part of the Yenisey-Khatanga Depression (Afanasenkov et al., 2016) to be a consequence of erosion, rather than original depositional pinching-out of Mesozoic clastic rocks against the basin margin.

6. Conclusions

Our combined structural and thermochronological studies resulted in the following conclusions:

1. NW-vergent thrusts and folds are widely distributed throughout the Southern Taimyr Domain and are reported from the Central Taimyr Domain as well. Outcrop-scale bedding-parallel thrusts preceded the main deformation stage, although major folds within the Tsvetkova Cape area were formed during the final stage of deformation.

2. The intense late Paleozoic deformations are recognized in a relatively narrow zone including the south-east margin of the Kara Terrane and adjacent parts of the Central Taimyr Domain, suggesting juxtaposition of the Kara Terrane and Siberian Craton by displacement along strike-slip faults. However, tectonic structures formed in the late Paleozoic were significantly overprinted during the latest Triassic – earliest Jurassic tectonic event and are difficult to interpret in the modern structural framework.

3. No evidence of significant late Paleozoic – Triassic deformation is recognized in the Southern Taimyr Domain. The modern structural style was formed during a deformation event dated by the widespread latest Triassic – earliest Jurassic unconformity and a cooling event at ca. 192 ± 11 Ma. The structural style was further modified during subsequent Cretaceous tectonic events, estimated by cooling ages at ca. 120 ± 6 Ma and 100-60 Ma.

4. The latest Triassic – earliest Jurassic tectonic event strongly modified pre-existing structures of the Northern and Central Taimyr domains and led to complete resetting of AFT ages in several samples. However, Ar-Ar muscovite ages do not show any resetting, suggesting an upper temperature limit for heating of the metamorphic rocks of < 300 °C. The latest Triassic – earliest Jurassic tectonic event correlates well with a synchronous tectonic event recorded in the Novaya Zemlya archipelago.

5. The Cretaceous tectonic events at ca. 120 ± 6 Ma and 100-60 Ma are best documented in the southern part of the Southern Taimyr Domain and the southern part of the Yenisey-Khatanga Depression, adjacent to the Olenek FZ. These events can be correlated to synchronous tectonic events in the Verkhoyansk FTB to the east.

6. A wide belt with predominantly late Mesozoic deformations frame the north-western, northern and eastern margins of the Siberian Craton. A complicated sequence of dextral and sinistral strike-slip displacements, recorded along the main thrusts within the Southern Taimyr Domain, result from a complex interplay between the Taimyr-Severnaya Zemlya FTB with the Pai-Khoi – Novaya Zemlya and Verkhoyansk fold and thrust belts located to the west and east respectively in the Mesozoic.

Acknowledgement

The fieldwork and analytical studies done in 2005–2012 were supported by projects with A.P.Karpinsky Russian Geological Research Institute (VSEGEI), TGS, Clapton Research Ltd., and Saint-Petersburg State University. Samples 50-10, 102-4, 624-6, and 625-6 were made available by A.A.Makariev. Interpretation of structural and thermochronological data was supported by the Russian Science Foundation grant № 17-17-01171. S.V.Malyshev acknowledges the President grant MK-739.2017. Discussions with A. Ivanov, J. Barnet and constructive reviews by S. Drachev and H. Lorenz significantly improved the manuscript.

Appendix A. Supplementary data

Supplementary data associated with this article can be found, in the online version, at https://doi.org/10.1016/j.jog.2018.02.002.

References

Afanasenkov, A.P., Nikishin, A.M., Unger, A.V., Bordunov, S.I., Lugovaya, O.V., Chikishev, A.A., Yakovishina, E.V., 2016. The tectonics and stages of the geological history of the Yenisei–Khatanga Basin and the conjugate Taimyr Orogen. Geotectonics 50, 161–178.

Alexandre, P., 2012. Comparison between grain size and multi-mineral $^{40}Ar/^{39}Ar$ thermochronology. Geochim. Cosmochim. Acta 75, 4260–4272.

Allmendinger, R.W., Cardozo, N.C., Fisher, D., 2012. Structural Geology Algorithms: Vectors & Tensors. Cambridge University Press, Cambridge, England.

Bezzubtsev, V.V., Malitch, N.S., Markov, F.G., Pogrebitsky Yu.E., 1983. Geological map of Gorny Taimyr 1:500000. Krasnoyarskgeologia, Krasnoyarsk (in Russian).

Bezzubtsev, V.V., Zalyaleev, R.Sh., Sakovich, A.B., 1986. Geological map of Gorny Taimyr 1:500000, explanatory note. Krasnoyarskgeologia, Krasnoyarsk (in Russian).

Corfu, F., Polteau, S., Planke, S., Faleide, J.I., Svensen, H., Zayoncheck, A., Stolbov, N., 2013. U-Pb geochronology of Cretaceous magmatism on Svalbard and Franz Josef Land: Barents Sea large igneous province. Geol. Mag. 150, 1127–1135.

Curtis, M.L., Lopez-Mir, B., Scott, R.A., Howard, J.P., 2018. Early Mesozoic sinistral transpression along the Pai-Khoi-Novaya Zemlya fold-thrust belt, Russia. Circum-Arctic Lithosphere Evolution 460. Geological Society, London, pp. 355–370. http://dx.doi.org/10.1144/SP460.2.

Dagys, A.S., Kazakov, A.M. 1984. Stratigraphy, Lithology and Cyclicity of Triassic Deposits in Northern Central Siberia. Transactions of Inst. Geol. Geophys. SB AcSci USSR 586. Novosibirsk, Nauka (in Russian).

Donelick, R.A., O'Sullivan, P.B., Ketcham, R.A., 2005. Apatite fission-track analysis. Rev. Mineral. Geochem. 58, 49–94.

Drachev, S.S., Shkarubo, S.I., 2018. Tectonics of the Laptev Shelf, Siberian Arctic. In: Pease, V., Coakley, B. (Eds.), Circum-Arctic Lithosphere Evolution. Geological Society, London, pp. 263–283. http://dx.doi.org/10.1144/SP460.15.

Drachev, S.S., Savostin, L.A., Groshev, V.G., Bruni, I.E., 1998. Structure and Geology of the continental shelf of the Laptev Sea, Eastern Russian Arctic. Tectonophysics 298, 357–393.

Drachev, S.S., Malyshev, N.A., Nikishin, A.M., 2010. Tectonic history and petroleum geology of the Russian Arctic Shelves: an overview. In: Vining, B.A., Pickering, S.C. (Eds.), Petroleum Geology: From Mature Basins to New Frontiers – Proceedings of the 7th Petroleum Geology Conference. Geological Society London, pp. 591–619.

Drachev, S.S., 2011. Tectonic setting, structure and petroleum geology of the Siberian Arctic offshore sedimentary basins. In: In: Spencer, A.M., Embry, A.F., Gautier, D.L., Stoupakova, A.V., Sørensen, K. (Eds.), Arctic Petroleum Geology 35. Geological Society London, Memoirs, pp. 369–394.

Drachev, S.S., 2016. Fold belts and sedimentary basins of the Eurasian Arctic. Arktos 2, 21.

Ershova, V.B., Prokopiev, A.V., Khudoley, A.K., 2015a. Integrated provenance analysis of Carboniferous deposits from Northeastern Siberia: implication for the late Paleozoic history of the Arctic. J. Asian Earth Sci. 109, 38–49.

Ershova, V.B., Prokopiev, A.V., Nikishin, V.A., Khudoley, A.K., Malyshev, N.A., Nikishin, A.M., 2015b. New data on Upper Carboniferous – Lower Permian deposits of Bol'shevik Isl. (Severnaya Zemlya Archipelago). Polar Res. 34, 24558. http://dx.doi.org/10.3402/polar.v34.24558.

Ershova, V., Prokopiev, A., Khudoley, A., Shneider, G., Andersen, T., Kullerud, K., Makar'ev, A., Maslov, A., Kolchanov, D., 2015c. Results of U-Pb (LA-ICPMS) dating of detrital zircons from metaterrigenous rocks of the basement of the North Kara basin. Dokl. Earth Sci. 464, 997–1000.

Ershova, V.B., Prokopiev, A.V., Khudoley, A.K., 2016a. Devonian-Permian sedimentary basins and paleogeography of the Eastern Russian Arctic: an overview. Tectonophysics 691, 234–255.

Ershova, V.B., Khudoley, A.K., Prokopiev, A.V., Tuchkova, M.I., Fedorov, P.V., Kazakova, G.G., Shishlov, S.B., O'Sullivan, P., 2016b. Trans-Siberian Permian Rivers: a key to understanding Arctic sedimentary provenance. Tectonophysics 691, 220–233.

Ershova, V., Anfinson, O., Prokopiev, A., Khudoley, A., Stockli, D., Faleide, J.-I., Gaina, C., Malyshev, N., 2018. Detrital Zircon (U-Th)/He Ages from Paleozoic Strata of the Severnaya Zemlya Archipelago: Deciphering Multiple Episodes of Paleozoic Tectonic Evolution within the Russian High Arctic. J. Geodyn (this issue).

Estrada, S., Henjes-Kunst, F., 2013. ^{40}Ar-^{39}Ar and U-Pb dating of Cretaceous continental rift-related magmatism on the northeast Canadian Arctic margin. Zeitschrift der Deutschen Gesellschaft für Geowissenschaften 164, 107–130.

Evenchick, C.A., Davis, W.J., Bedard, J.H., Hayward, N., Friedman, R.M., 2015. Evidence for protracted High Arctic large igneous province magmatism in the central Sverdrup Basin from stratigraphy geochronology, and paleodepths of saucer-shaped sills. GSA Bull. 127, 1366–1390.

Fitzgerald, P.G., Gleadow, A.J.W., 1988. Fission track geochronology, tectonics and structure of the Transantarctic Mountains in northern Victoria Land, Antarctica. Chem. Geol. (Isotope Geology Section) 73, 169–198.

Franke, D., Reichert, C., Damm, V., Piepjohn, K., 2008. The South Anyui suture, Northeast Arctic Russia, revealed by offshore seismic data. Norw. J. Geol. 88, 189–200.

Gee, D.G., Bogolepova, O.K., Lorenz, H., 2006. The Timanide, Caledonide and Uralide orogens in the Eurasian high Arctic, and relationships to the palaeo-continents Laurentia, Baltica and Siberia. In: In: Gee, D.G., Stephenson, R.A. (Eds.), 2006. European Lithosphere Dynamics 32. Geological Society London, Memoirs, pp.

507–520.
Gleadow, A.J.W., Duddy, I.R., Green, P.F., Lovering, J.F., 1986. Confined fission track lengths in apatite: a diagnostic tool for thermal history analysis. Contrib. Mineral. Petrol. 94, 405–415.
Glorie, S., Agostino, K., Dutch, R., Pawley, M., Hall, J., Danišik, M., Evans, N.J., Collins, A.S., 2017. Thermal history and differential exhumation across the Eastern Musgrave Province, South Australia: Insights from low-temperature thermochronology. Tectonophysics. http://dx.doi.org/10.1016/j.tecto.2017.03.003.
Green, P.F., Duddy, I.R., Laslett, G.M., Hegarty, K.A., Gleadow, A.J.W., Lovering, J.F., 1989. Thermal annealing of fission tracks in apatite 4, Quantitative modeling techniques and extension to geological timescales. Chem. Geol.: Isotope Geosci. Section 79, 155–182.
Green, P.F., 1986. On the thermo-tectonic evolution of Northern England: evidence from fission track analysis. Geol. Mag. 123, 493–506.
Inger, S., Scott, R., Golionko, B., 1999. Tectonic evolution of the Taimyr Peninsula northern Russia: implications for Arctic continental assembly. J. Geol. Soc. London 156, 1069–1072.
Jones, P.B., 1996. Triangle zone geometry: terminology and kinematics. Can. Soc. Petrol. Geol. Bull. 40, 139–152.
Ketcham, R.A., Donelick, R.A., Carlson, W.D., 1999. Variability of apatite fission-track annealing kinetics: III. Extrapolation to geological time scales. Am. Mineral. 84, 1235–1255.
Ketcham, R.A., Donelick, R.A., Donelick, M.B., 2000. AFTSolve: a program for multi-kinetic modeling of apatite fission-track data. Geol. Mater. Res. 2, 1–32.
Ketcham, R.A., 2005. Forward and inverse modeling of low-temperature thermochronometry data. Rev. Mineral. Geochem. 58, 275–314.
Khudoley, A.K., Prokopiev, A.V., 2007. Defining the eastern boundary of the North Asian craton from structural and subsidence history studies of the Verkhoyansk fold-and-thrust belt. In: In: Sears, J.W., Harms, T.A., Evenchick, C.A. (Eds.), Whence the Mountains? Inquiries into the Evolution of Orogenic Systems: A Volume in Honor of Raymond A. Price 433. Geological Society of America, pp. 391–410 Special Papers.
Khudoley, A., Chamberlain, K., Ershova, V., Sears, J., Prokopiev, A., MacLean, J., Kazakova, G., Malyshev, S., Molchanov, A., Kullerud, K., Toro, J., Miller, E., Veselovskiy, R., Li, A., Chipley, D., 2015. Proterozoic supercontinental restorations: Constraints from provenance studies of Mesoproterozoic to Cambrian clastic rocks, eastern Siberian Craton. Precamb. Res. 259, 78–94.
Kontorovich, V.A., 2011. The tectonic framework and hydrocarbon prospectivity of the western Yenisei–Khatanga regional trough. Russ. Geol. Geophys. 52, 804–824.
Koppers, A.A.P., 2002. ArArCALC-software for 40Ar/39Ar age calculations. Comput. Geosci. 28, 605–619.
Korago, E.A., Timofeeva, T.N., 2005. Magmatism of the Novaya Zemlya (in Context of Geological History of the Barents − Severnaya Kara Region). VNIIO Press, Saint Petersburg in Russian.
Kuptsova, A.V., Khudoley, A.K., Davis, W., Rainbird, R.H., Molchanov, A.V., 2015. Results of the U-Pb age of detrital zircons from Upper Proterozoic deposits of the eastern slope of the Anabar uplift. Stratigr. Geol. Correl. 23, 246–261.
Kurapov, M.Yu., Ershova, V.B., Makariev, A.A., Makarieva, E.M., Khudoley, A.K., Luchitskaya, M.V., Prokopiev, A.V., 2018. Carboniferous granitoid magmatism of Northern Taimyr: results of isotopic-geochemical study and geodynamic interpretation. Geotectonics 52 in press.
Lisker, F., Ventura, B., Glasmacher, U.A., 2009. Apatite thermochronology in modern geology. In: In: Lisker, F., Ventura, B., Glasmacher, U.A. (Eds.), Thermochronological Methods: From Palaeotemperature Constraints to Landscape Evolution Models 324. Geological Society, London, pp. 1–23 Special Publications.
Lopatin, B.G., Pavlov, L.G., Orgo, V.V., Shkarubo, S.I., 2001. Tectonic Structure of Novaya Zemlya. Polarforschung 69, 131–135.
Lorenz, H., Gee, D.G., Whitehous, M., 2007. New geochronological data on Palaeozoic igneous activity and deformation in the Severnaya Zemlya Archipelago Russia, and implications for the development of the Eurasian Arctic margin. Geol. Mag. 144, 105–125.
Lorenz, H., Gee, D.G., Simonetti, A., 2008. Detrital zircon ages and provenance of the Late Neoproterozoic and Palaeozoic successions on Severnaya Zemlya: Kara Shelf: a tie to Baltica. Norw. J. Geol. 88, 235–258.
Makariev, A.A., Makarieva, E.M., 2011. Geological Map of Russian Federation, scale 1:1000000, T-45–48 (Cape Chelyuskin). VSEGEI, St. Petersburg in Russian.
Makariev, A.A., 2013. Geological Map of Russian Federation, Scale 1:1000000, T-45–48 (Cape Chelyuskin). Explanatory Notes. VSEGEI, St. Petersburg in Russian.
Marrett, R.A., Allmendinger, R.W., 1990. Kinematic analysis of fault-slip data. J. Struct. Geol. 12, 973–986.
Metelkin, D.V., Vernikovsky, V.A., Kazansky, A.Y., Bogolepova, O.K., Gubanov, A., 2005. Palaeozoic history of the Kara microcontinent and its relation to Siberia and Baltica: Palaeomagnetism: palaeogeography and tectonics. Tectonophysics 398, 225–243.
Metelkin, D.V., Vernikovsky, V.A., Kazansky, A.Y., 2012. Tectonic evolution of the Siberian paleocontinent from the Neoproterozoic to the Late Mesozoic: paleomagnetic record and reconstructions. Russ. Geol. Geophys. 39, 791–794.
Migai I.M. 1952. Geological structure of the Cape Tsvetkov area in the east Taimyr. Transactions of the Institute of Geology of Arctic, 36. Leningrad-Moscow, Glavsevmorput (in Russian).
Morley, C.K., 1986. A classification of thrust fronts. AAPG Bull. 70, 12–25.
Nikitenko, B.L., Shurygin, B.N., Knyazev, V.G., Meledina, S.V., Dzyuba, O.S., Lebedeva, N.K., Peshchevitskaya, E.B., Glinskikh, L.A., Goryacheva, A.A., Khafaeva, S.N., 2013. Jurassic and Cretaceous stratigraphy of the Anabar area (Arctic Siberia: Laptev Sea coast) and the Boreal zonal standard. Russ. Geol. Geophys. 54, 808–837.
O'Sullivan, P.B., Parrish, R.R., 1995. The importance of apatite composition and single-grain ages when interpreting fission track data from plutonic rocks: a case study from the Coast Ranges, British Columbia. Earth Planet. Sci. Lett. 132, 213–224.
O'Sullivan, P.B., Orr, M., O'Sullivan, A.J., Gleadow, A.J.W., 1999. Episodic Late Paleozoic to Cenozoic denudation of the southeastern highlands of Australia: evidence from the Bogong Hill Plains, Victoria. Aust. J. Earth Sci. 46, 199–216.
Pease, V., Scott, R., 2009. Crustal affinities in the Arctic Uralides: northern Russia: significance of detrital zircon ages from Neoproterozoic and Palaeozoic sediments in Novaya Zemlya and Taimyr. J. Geol. Soc. 166, 517–527.
Pease, V., Gee, D., Vernikovsky, V., Vernikovskaya, A., Kireev, S., 2001. Geochronological evidence for late Grenvillian magmatic and metamorphic events in central Taimyr northern Siberia. Terra Nova 13, 270–280.
Pease, V., 2011. Eurasian orogens and Arctic tectonics: an overview. In: In: Spencer, A.M., Embry, A.F., Gautier, P.L., Stoupakova, A.V., Soerensen, K. (Eds.), Arctic Petroleum Geology 35. Geological Society London, Memoirs, pp. 311–324.
Geological Map of Russia and Adjoining Water Areas, Scale 1:2500000. In: Petrov, O.V. (Ed.), Ministry of Natural Resources and Ecology, St. Petersburg.
Pogrebitsky, Yu.E., Shanurenko, N.K., 1998. Explanatory Note to Geological Map S-47-49 of Russian Federation (Lake Taimyr). VSEGEI, St. Petersburg in Russian.
Pogrebitsky, Yu.E., 1971. Paleotectonic Analysis of the Taimyr Folded System. Nedra, Leningrad in Russian.
Pogrebitsky, Yu.E., 1998. Geological Map S-47-49 of Russian Federation (Lake Taimyr). VSEGEI, St. Petersburg in Russian.
Priyatkina, N., Collins, W.J., Khudoley, A., Zastrozhnov, D., Ershova, V., Chambarlain, K., Shatsillo, A., Proskurnin, V., 2017. The Proterozoic evolution of northern Siberian Craton margin: A comparison of U-Pb-Hf signatures from sedimentary units of the Taimyr orogenic belt and the Siberian platform. Int. Geol. Rev. http://dx.doi.org/10.1080/00206814.2017.1289341.
Prokopiev, A.V., Deikunenko, A.V., 2001. Deformational structures of fold-and-thrust belts. In: Parfenov, L.M., Kuzmin, M.I. (Eds.), Tectonics, Geodynamics and Metallogeny of the Sakha Republic (Yakutia). MAIK Nauka/Interperiodica, Moscow, pp. 156–198 in Russian.
Prokopiev, A., Ershova, V., Khudoley, A., Anfinson, O., Stockli, D., Faleide, J.I., Gaina, C., Sobolev, N., Petrov, E. 2016. Structural Analysis and Detrital Zircon (U-Th)/He Ages from Paleozoic Strata of the NW Novaya Zemlya Archipelago (Russian High Arctic). Geological Society of America Abstracts with Programs, Vol. 48, No. 7, Abstract No: 285900. 10.1130/abs/2016AM-285900.
Pronkin, A.R., Savchenko, V.J., Khlebnikov, P.A., Ernst, V.A., Filiptsov, Yu.A., Afanasenkov, A.P., Efimov, A.S., Stupakova, A.V., Bordunov, S.I., Suslova, A.A., Sautkin, R.S., Glukhova, T.A., Peretolchin, K.A., 2012. New data about geological structure and possible oil and gas potential of the West-Siberian and Siberian platform joining zone with folded Taimyr. Oil and Gas Geology 1, 28–42 in Russian.
Proskurnin, V.F., Schneider, G.V., Bagaeva, A.A., Borisenkov, K.V., 2016. Geological Map S-48-I, II of Russian Federation. VSEGEI, St. Petersburg Scale 1:200 000, 1 sheet (in press) (In Russian).
Proskurnin, V.F., 2009a. Geological Map of the Russian Federation, Scale 1: 1000000, S-48 (Lake Taimyr). VSEGEI, St. Petersburg in Russian.
Proskurnin, V.F., 2009b. Explanatory Note to Geological Map S-48 of the Russian Federation (Lake Taimyr). VSEGEI, St. Petersburg scale 1: 1 000 000. (in Russian).
Puchkov, V.N., 2009. The evolution of the Uralian orogen. In: In: Murphy, J.B., Keppie, J.D., Hynes, A.J. (Eds.), Ancient Orogens and Modern Analogues 327. Geological Society, London, pp. 161–195 Special Publications.
Puchkov, V.N., 2010. Geology of the Urals and Cis-Urals (actual Problems of Stratigraphy, Tectonics, Geodynamics and Metallogeny). DesignPoligraphService, Ufa in Russian.
Reiners, P.W., Ehlers, T.A., Zeitler, P.K., 2005. Past present, and future of thermochronology. Rev. Mineral. Geochem. 58, 1–18.
Samygin, S.G., 2012. Vendian nappes and tectonic evolution of Taimyr in Late Precambrian. Bull. Moscow Soc. Nat. (Bulletin MOIP), Geol. Ser 4, 3–19 in Russian.
Samygin, S., 2015. Neoproterozoic tectonic evolution of the Taimyr Peninsula (Arctic Asia): An example of a Late Precambrian thrust-fold belt. Episodes 38, 39–48.
Scott, R.A., Howard, J.P., Guo, L., Schekoldin, R., Pease, V., 2010. Offset & curvature of the Novaya Zemlya fold-and-thrust belt, Arctic Russia. In: Vining, B.A., Pickering, S.C. (Eds.), Petroleum Geology: From Mature Basins to New Frontiers − Proceedings of the 7th Petroleum Geology Conference. Geological Society, London, pp. 645–657.
Smith, M.E., Singer, B., Carroll, A., 2003. $^{40}Ar/^{39}Ar$ geochronology of the Eocene Green River Formation, Wyoming. Geol. Soc. Am. Bull. 115, 549–565.
Uflyand, A.K., Natapov, L.M., Lopatin, V.M., Chernov, D.V., 1991. The tectonic nature of the Taymyr Peninsula. Geotectonics 25, 512–523.
Vermeesch, P., 2009. RadialPlotter: a Java application for fission track, luminescence and other radial plots. Radiat. Meas. 44 (4), 409–410.
Vernikovsky, V.A., Vernikovskaya, A.E., 2001. Central Taimyr accretionary belt (Arctic Asia): meso-neoproterozoic tectonic evolution and Rodinia breakup. Precambrian Res. 110, 127–141.
Vernikovsky, V.A., Sal'nikova, E.B., Kotov, A.B., Ponomarchuk, V.A., Kovach, V.P., Travin, A.V., Yakovleva, S.Z., Berezhnaya, N.G., 1998. Age of postcollision granitoids, northern taimyr: U–Pb, Sm–Nd, Rb–Sr and Ar–Ar data. Dokl. Earth Sci. 363, 375–378 in Russian.
Vernikovsky, V.A., Pease, V.L., Vernikovskaya, A.E., Romanov, A.P., Gee, D.G., Travin, A.V., 2003. First report of early Triassic A-type granite and syenite intrusions from Taimyr: product of the northern Eurasian superplume? Lithos 66, 23–36.
Vernikovsky, V.A., Vernikovskaya, A.E., Pease, V.L., Gee, D., 2004. Neoproterozoic orogeny along the margins of Siberia. In: In: Gee, D.G. (Ed.), The Neoproterozoic Timanide Orogen of Eastern Baltica 30. Geological Society London, Memoirs, pp. 233–248.
Vernikovsky, V., Metelkin, D., Vernikovskaya, A., Sal'nikova, E., Kovach, V., Kotov, A., 2011. The oldest island arc complex of Taimyr: concerning the issue of the Central-Taimyr accretionary belt formation and palaeogeodynamic reconstructions in the Arctic. Dokl. Earth Sci. 436, 186–192.
Vernikovsky, V.A., 1996. Geodynamic Evolution of Taimyr Fold Area. SB RAS,

Novosibirsk in Russian.
Verzhbitsky, V., Khudoley, A., 2010. Western Laptev Sea region framework: structural style and timing of deformation. EAGE. In: 4th Saint Petersburg International Conference & Exhibition. 5-8 April 2010 Paper A08E. 5 p.
Zhang, X., Omma, J., Pease, V., Scott, R., 2013. Provenance of late Paleozoic–Mesozoic sandstones, Taimyr peninsula, the Arctic. Geosciences 3, 502–527.
Zhang, X., Pease, V., Skogseid, J., Wohlgemuth-Ueberwasser, C., 2016. Reconstruction of tectonic events on the northern Eurasia margin of the Arctic, from U-Pb detrital zircon provenance investigations of late Paleozoic to Mesozoic sandstones in southern Taimyr Peninsula. Geol. Soc. Am. Bull. 128, 29–46.
Zhang, X., Pease, V., Carter, A., Kostuychenko, S., Suleymanov, A., Scott, R., 2018. Timing of exhumation and deformation across the Taimyr fold-thrust belt: insights from apatite fission track dating and balanced cross-sections. In: In: Pease, V., Coakley, B. (Eds.), Circum-Arctic Lithosphere Evolution 460. Geological Society, London, pp. 315–333.
Zonenshain, L.P., Kuzmin, M.I., Natapov, L.M., 1990. Geology of the USSR: a plate tectonic synthesis: american Geophysical Union. Geodynamics Series 21.